Natural Resources Canada | Ressources naturelles Canada

GEOLOGICAL SURVEY OF CANADA
OPEN FILE 8410

Geology and petrography of selected carbonate-hosted Zn-Pb deposits of the southeastern Cordillera, British Columbia and Alberta

N. Drage and S. Paradis

2018

Canada

GEOLOGICAL SURVEY OF CANADA
OPEN FILE 8410

Geology and petrography of selected carbonate-hosted Zn-Pb deposits of the southeastern Cordillera, British Columbia and Alberta

N. Drage and S. Paradis

2018

Permanent link: https://doi.org/10.4095/311220

This publication is available for free download through GEOSCAN (http://geoscan.nrcan.gc.ca/)

Recommended citation
Drage, N. and Paradis, S., 2018. Geology and petrography of selected carbonate-hosted Zn-Pb deposits of the southeastern Cordillera, British Columbia and Alberta; Geological Survey of Canada, Open File 8410, 29 p. https://doi.org/:10.4095/311220

Publications in this series have not been edited; they are released as submitted by the author.

TABLE OF CONTENTS

Figures

Geology and petrography of selected carbonate-hosted Zn-Pb deposits of the southeastern Cordillera, British Columbia and Alberta

N. Drage[1] and S. Paradis[2*]

[1]Natashiadrage@gmail.com
[2]Geological Survey of Canada, Natural Resources Canada NRCan - Geological Survey of Canada, 9860 West Saanich Road, Sidney, British Columbia V8L 4B2
*Corresponding author's email: suzanne.paradis@canada.ca

ABSTRACT

The Monarch, Kicking Horse, Shag, Munroe, and Oldman carbonate-hosted, sulphide deposits of the southeastern Canadian Cordillera share many of the characteristics of Mississippi Valley-type deposits, such as stratabound lenses, pods, and disseminated sulphide minerals locally accompanied by breccia-vein systems. The deposits are hosted in dolostone located at major facies transitions between shallow-water carbonate platformal and deeper basinal rocks along the ancient Paleozoic margin of the Canadian Cordillera. They are associated with fault and breccia structures located nearby or along the platform-basin facies transition. The location and geometry of these deposits reflect the interplay between structures (i.e. deep-seated faults located at platform-basin transition) and lithologies (i.e. permeable and reactive stratigraphic units).

Sulphides, consisting of sphalerite, galena, and, to a lesser extent, pyrite, are present as fracture, breccia matrix, and vug-fillings, as well as replacement of dolostone host rock. Dolomite and calcite are the common gangue minerals. Quartz is present at three showings of the Shag deposit but is otherwise absent (except for trace amounts at Kicking Horse). Paragenesis is relatively simple and shares many features across the studied deposits. Generally, sulphide paragenesis starts with pyrite, followed by sphalerite and then galena.

INTRODUCTION

Mississippi Valley-type (MVT) sulphide deposits of the southeastern Canadian Cordillera are under investigation as part of the Government of Canada's Targeted Geoscience Initiative to examine the links among various types of carbonate-hosted mineralization, including MVT, carbonatite-related REE (±fluorite), and magnesite deposits. This paper reports on five carbonate-hosted Zn-Pb deposits (Monarch, Kicking Horse, Shag, Munroe, and Oldman) in the Rocky Mountains (Fig. 1), providing preliminary data, which in the future will be supplemented by mineralogical, isotopic (i.e. O, C, Sr, S, Pb), and fluid inclusion analyses. Fieldwork and sampling of the Monarch, Kicking Horse, and Munroe deposits occurred in 2016 (Paradis and Simandl, 2017), with samples from the Oldman and Shag deposits provided by Roy Eccles (Apex Geoscience Ltd.) and Chris Graf (Spectrum Mining Corporation), respectively.

The deposits are in a 'carbonate corridor' that extends northward in the Rocky Mountain Foreland Belt of the Canadian Cordillera (Fig. 1). Fieldwork in 2016 examined the southeastern portion of the carbonate corridor, segments of which host numerous MVT deposits, along with other deposit types, such as SEDEX, carbonatite, hydrothermal REE-fluorite and polymetallic veins, and a variety of industrial mineral deposits including replacement and vein barite (± fluorite, ± sulphides), magnesite, gypsum, and talc. To date, the Monarch, Kicking Horse, and Oldman deposits have been the focus of a number of studies (Goranson, 1937; Ney, 1954; Evans et al., 1968; Holter, 1977; Salat, 1988; Nesbitt and Muehlenbachs, 1994; Nesbitt and Prochaska, 1998; Symons et al., 1998; Pana, 2006; Vandeginste et al., 2007), whereas the Shag and Munroe deposits have received little or no attention (Bending, 1979; Gibson, 1979a,b; Lenters, 1981, 1982; Jensen, 1991).

REGIONAL GEOLOGICAL AND TECTONIC SETTING

The carbonate-hosted deposits studied in this paper are located in the Main and Front ranges of the southern Rocky Mountain Foreland Belt (Fig. 1). This terrane is a thin-skinned thrust-and-fold belt that formed along a basal-detachment fault system initiated by eastward accretion of allochthonous terranes in the Jurassic to Early Tertiary (McMechan, 2012). This deformation exposed rocks of the Upper Proterozoic to Upper Jurassic miogeocline-platform that formed on the western margin of the North American craton. Upper Proterozoic to Lower Cambrian rocks of the Windermere Supergroup (Fig. 2) formed during intra-

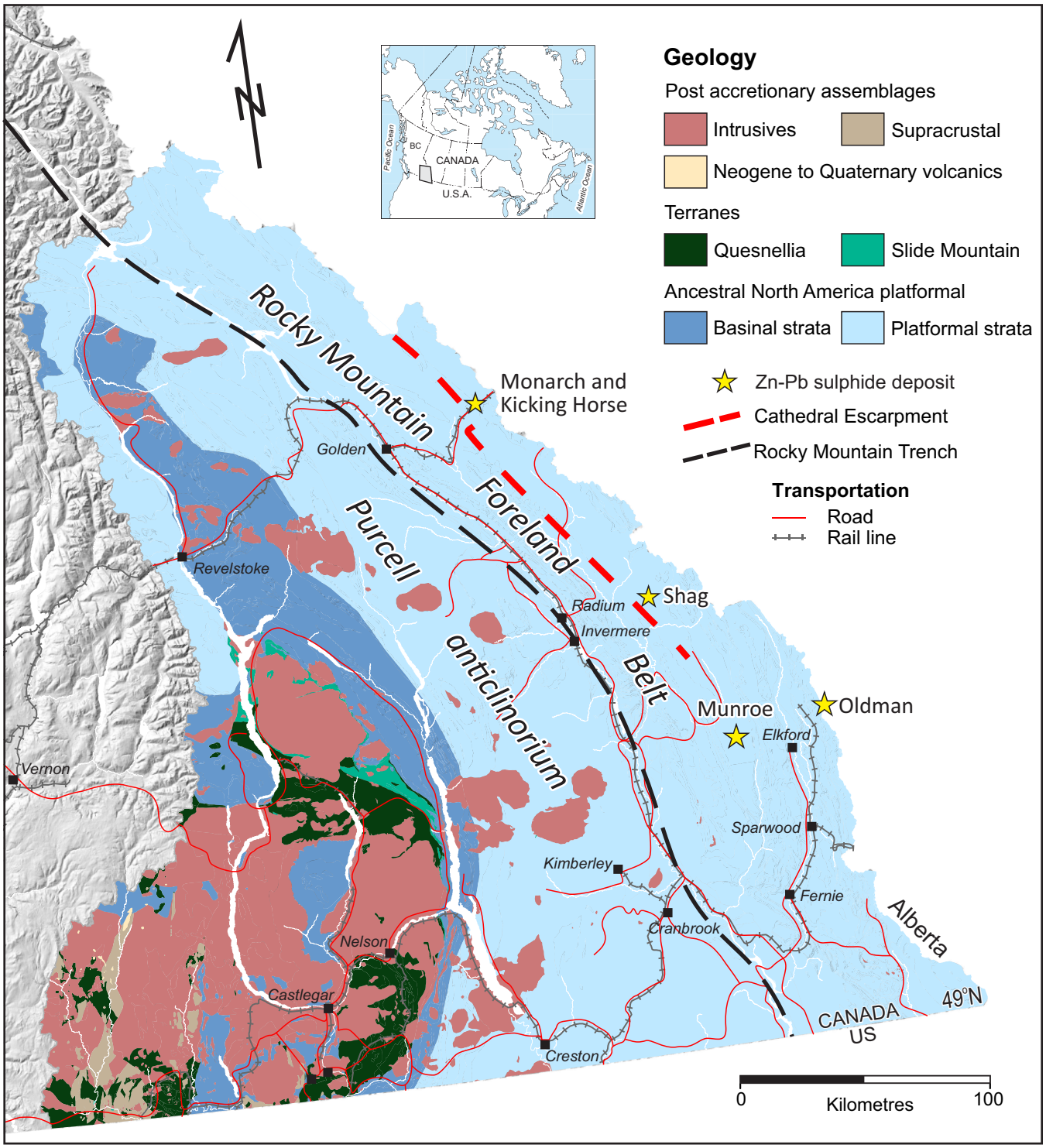

Figure 1. Regional geological map of southeastern British Columbia showing locations of the Zn-Pb sulphide deposits studied. Note that the Oldman deposit is located in Alberta. The projection of the Cathedral Escarpment corresponds approximately to the location of the Kicking Horse Rim, a paleogeographic high that was initiated in the early Middle Cambrian and persisted into the Ordovician (Aitken, 1971, 1989). Both mark the transition from shallow-water carbonate to the east and basinal slope lithofacies to the west during the early Paleozoic. Modified from Katay (2017). Terranes are from British Columbia digital geology map (Cui et al., 2015).

continental rifting (Price, 1994), and were followed by Middle Cambrian platform-basin transition sequences that formed around a paleogeographic high known as the Kicking Horse Rim (Aitken, 1971, 1989). This margin, which corresponds approximately to the projection of the Cathedral Escarpment (shown on Fig. 1), and other escarpments, moved laterally during the early Paleozoic. A number of MVT, SEDEX, magne-

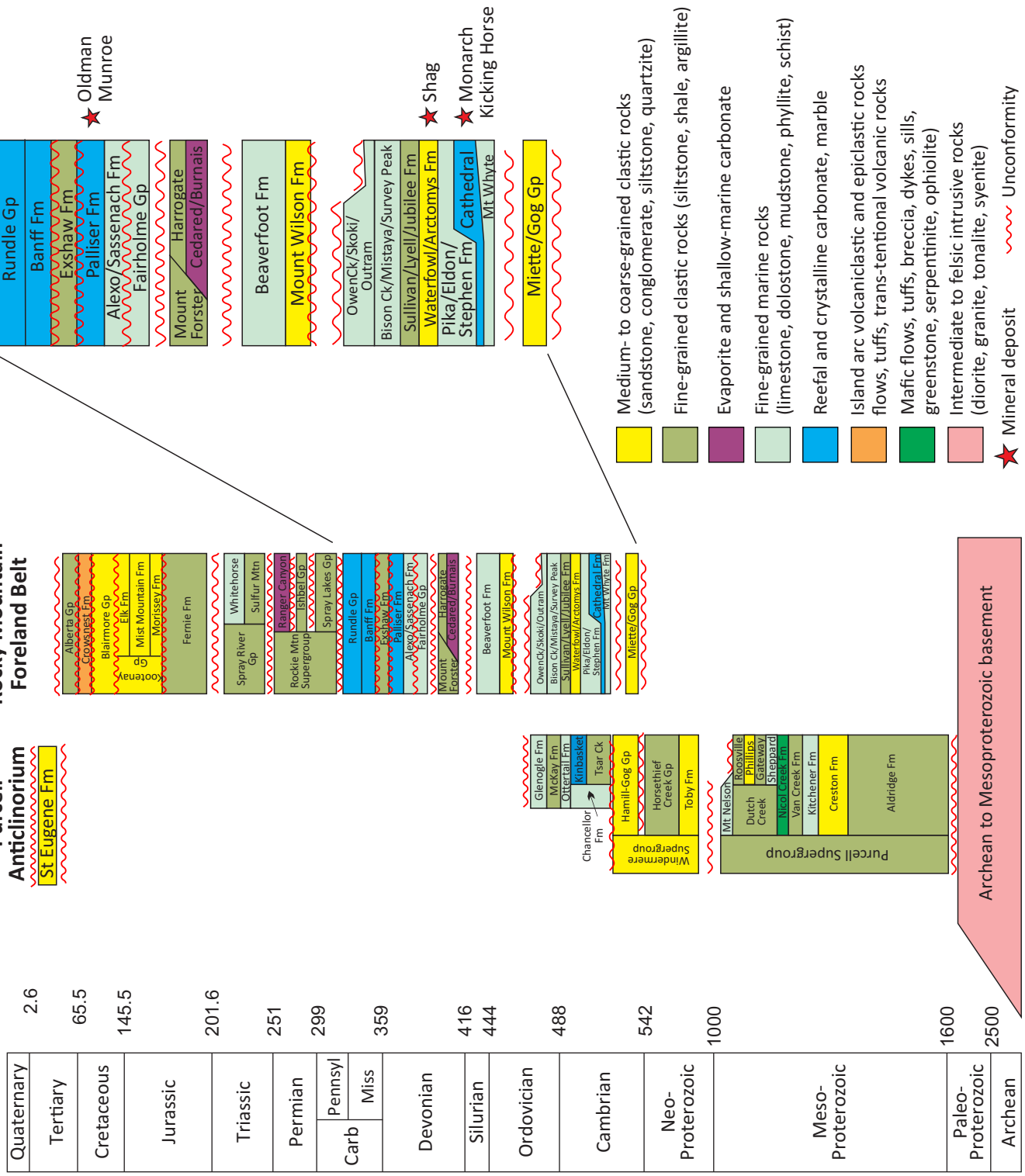

Figure 2. Generalized stratigraphy of the Purcell anticlinorium and the Rocky Mountain Foreland Belt with locations of studied Zn-Pb sulphide deposits indicated by stars. Modified from Katay (2017). Abbreviations: Carb – Carboniferous; Fm – Formation; Gp – Group.; Pennsyl – Pennsylvanian; Miss – Mississippian

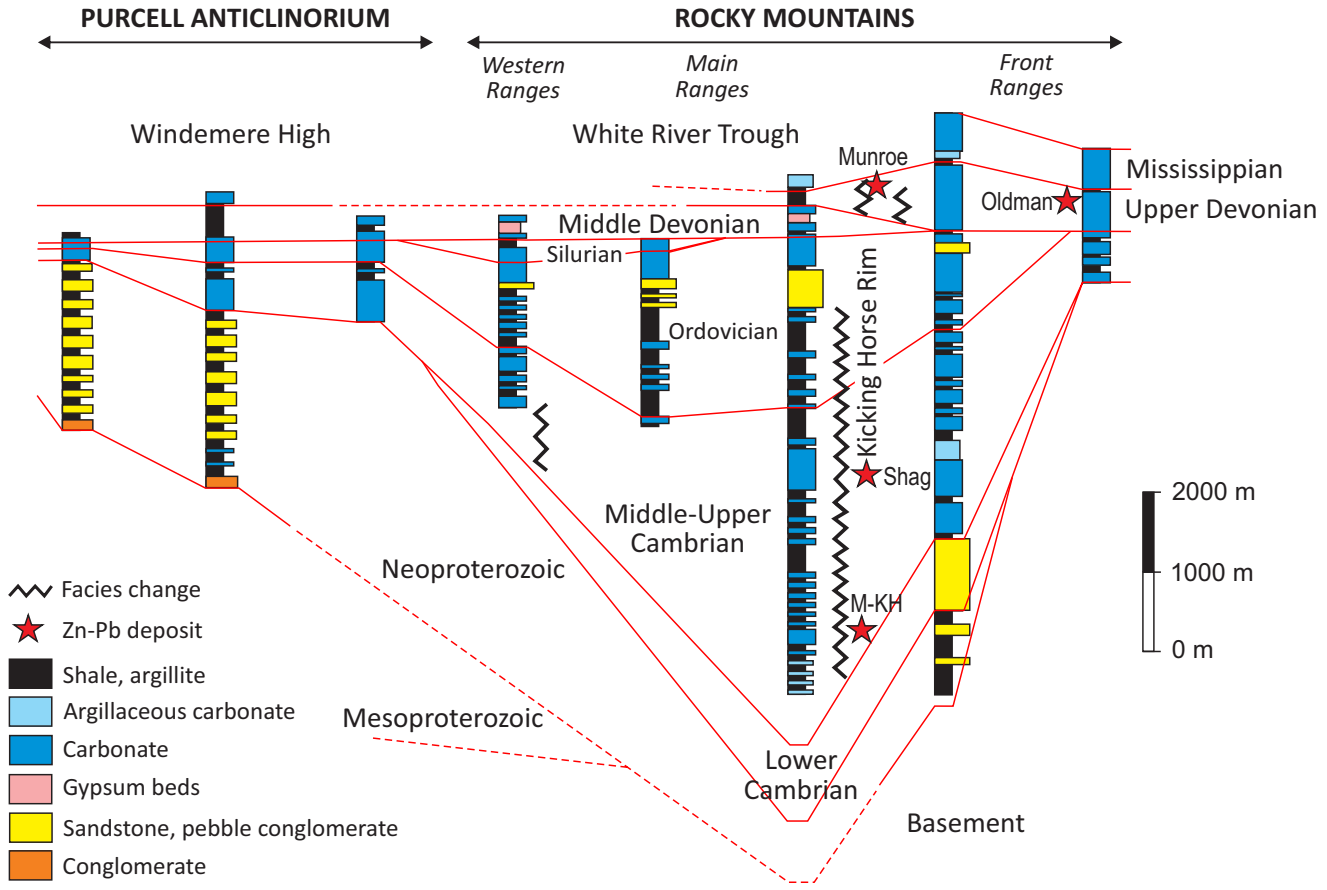

Figure 3. Approximately west-east stratigraphic cross-section of Proterozoic to Mississippian strata from the Purcell anticlinorium to the Rocky Mountains (southwest of Radium, British Columbia). Abbreviation: M-KH – Monarch-Kicking Horse. From McMechan and Macey (2012).

site, and talc deposits are located spatially along this facies transition margin (Simandl and Hancock, 1991; Simandl et al., 1992; Powell et al., 2006; McMechan, 2012; Paradis and Simandl, 2017, 2018). West of these escarpments lies the Chancellor Group basinal sequence, and to the east a series of platformal carbonate rocks that host many MVT deposits, including Monarch, Kicking Horse, and Shag. This tectono-sedimentary environment remained until the Middle Jurassic during which carbonates of the Cathedral and equivalent formations (hosting the Monarch, Kicking Horse, and Shag deposits), and carbonates of the Devonian Palliser Formation (hosting the Munroe and Oldman deposits) were deposited (Fig. 2). Following this period, Middle Jurassic to Eocene Cordilleran orogenic tectonism deformed, imbricated, and transported these sequences northeastward (McMechan, 2012).

GEOLOGY OF SELECTED CARBONATE-HOSTED Zn-Pb DEPOSITS

Monarch and Kicking Horse Deposits

The Monarch and Kicking Horse Zn-Pb (±Ag) deposits are located on the north and south slopes, respectively, of Mt. Stephen in the Yoho National Park, British Columbia (Goranson, 1937). The Monarch orebody was discovered in 1884 during construction of the Canadian Pacific Railway, with the Kicking Horse orebody discovered in the early 1900s. Since then, the deposits have been described by Allan (1914), Goranson (1937), Brown (1948), Ney (1954), and Evans et al. (1968), providing invaluable information on underground workings, morphology of orebodies, and lithological relationships. Pana (2006) re-examined the geological and structural settings of the deposits to assess the influence of stratigraphic and structural controls on the mineralization. Vandeginste et al. (2007) investigated the geochemistry of the ore-forming fluids to constrain ore-forming processes.

The now mined out Monarch and Kicking Horse deposits constitute several orebodies in a thick succession of massive to thin-bedded, brecciated, Middle Cambrian Cathedral Formation dolostone. The orebodies and associated breccias and dolomitized zones trend northerly, parallel to the Kicking Horse Rim, a fault-controlled, paleotopographic high over which a carbonate platform-to-basin facies transition occurred (Fig. 3; Aitken, 1971, 1997; McMechan and Macey, 2012). A footwall block bound by the Fossil Gully and

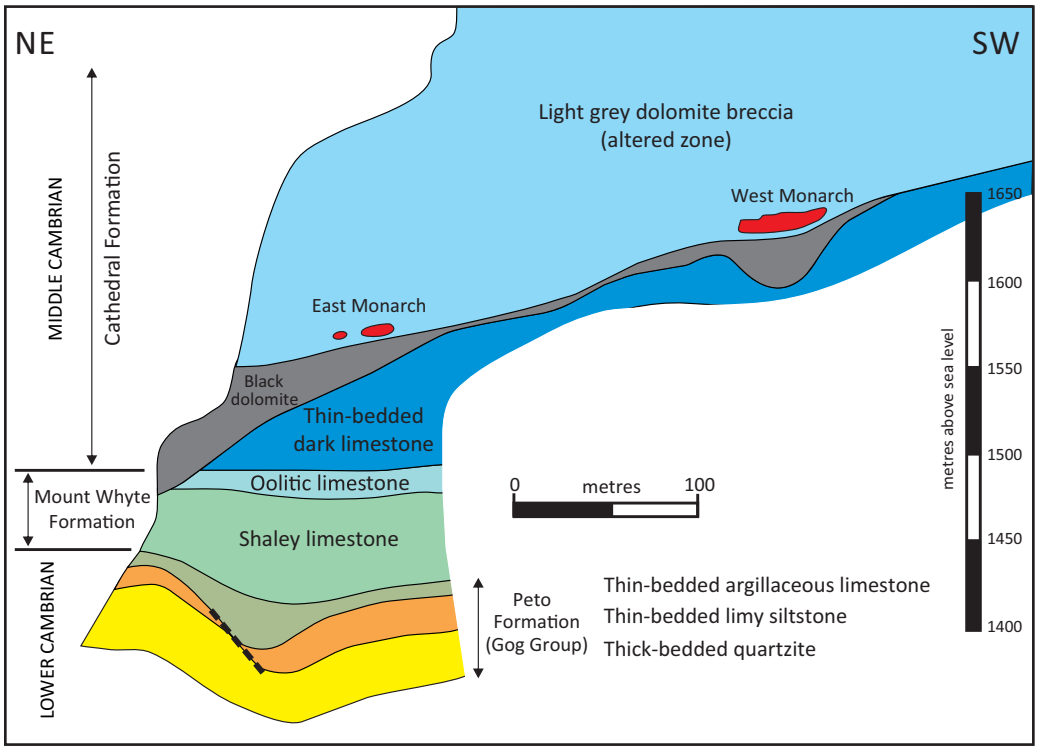

Figure 4. Northeast-southwest cross-section (looking south) of the Monarch orebodies (from Ney, 1954). Vertical scale refers to the elevation above sea level.

the Stephen-Cathedral normal faults confines the mineralized breccias (Vandeginste et al., 2007).

The orebodies lie on the northeast flank of a northwest-trending anticline that has an axis plunging northward at low angle (Cook, 1975). They form north-northwest-aligned concordant sulphide lenses near the base of a brecciated dolomitized alteration zone in the lower Cathedral Formation (Ney, 1957). The stratigraphic interval that hosts the orebodies is 60 m thick and occurs in the lower 125 m of the Cathedral Formation, just above the contact with a black dolostone (Fig. 4; Goranson, 1937; Brown, 1948; Hedley, 1954; Ney, 1957). The mineralization is preferentially hosted by the brecciated portion of the dolostone that consists of two rock types, a grey breccia and a white breccia (Ney, 1954). The grey breccia consists of light grey, angular to subangular and minor rounded fragments of variable size (≤1 cm to several metres in diameter) in a darker grey dolomite matrix. In this breccia, the fragments are typically lighter grey than the matrix, which can be almost black (Ney, 1954). The white breccia refers to a stockwork of abundant coarse-grained white dolomite veins cutting fragments and matrix of the light grey dolomite breccia. A non-mineralized version of this breccia is widespread in the Cathedral Formation (Ney, 1954).

Sulphide minerals at Monarch and Kicking Horse consist of galena, sphalerite and pyrite, and exhibit different styles of occurrence. Although minor chalcopyrite, barite, and native silver were reported by Goranson (1937), they were not observed in our samples. Most commonly, sulphides are disseminated in the cement of the grey breccias or form veinlets and aggregates in the white breccias. They also occur as host rock replacement. Ney (1957) mentioned the presence of sulphide minerals along bedding planes of the underlying black dolomitized limestone.

Shag Deposit

The Shag deposit consists of seventeen Zn-Pb (±Ag) showings in Middle to Upper Cambrian carbonate rocks (Jensen, 1991). This deposit was discovered in 1977 by Rio Tinto Canadian Exploration Ltd. under the 'Graf Lead-Zinc Reconnaissance Program'. Since then, work on the property has included prospecting, geological mapping, geochemical soil and silt sampling, induced polarization (IP) and resistivity surveys, and diamond drilling (Hendrickson, 1988; Jensen, 1991). Although stratigraphically higher than Monarch and Kicking Horse, the Shag deposit is also located in platformal carbonate along the Kicking Horse Rim (McMechan and Leech, 2011a), just east of the transition to basinal shale and limestone of the Middle to Upper Cambrian Chancellor Formation, along the Eldon Escarpment. The majority of showings are in dolostone of the Stephen, Eldon, and Waterfowl formations (Fig. 5) at or near the contact with overlying argillaceous limestone (Lenters, 1982).

The BM mineralized horizon occurs in a dolostone unit at the top of the Eldon Formation (unit C3 of Bending, 1979) and includes the BM, BM extension (float), BM Fracture, and Galena (float) showings

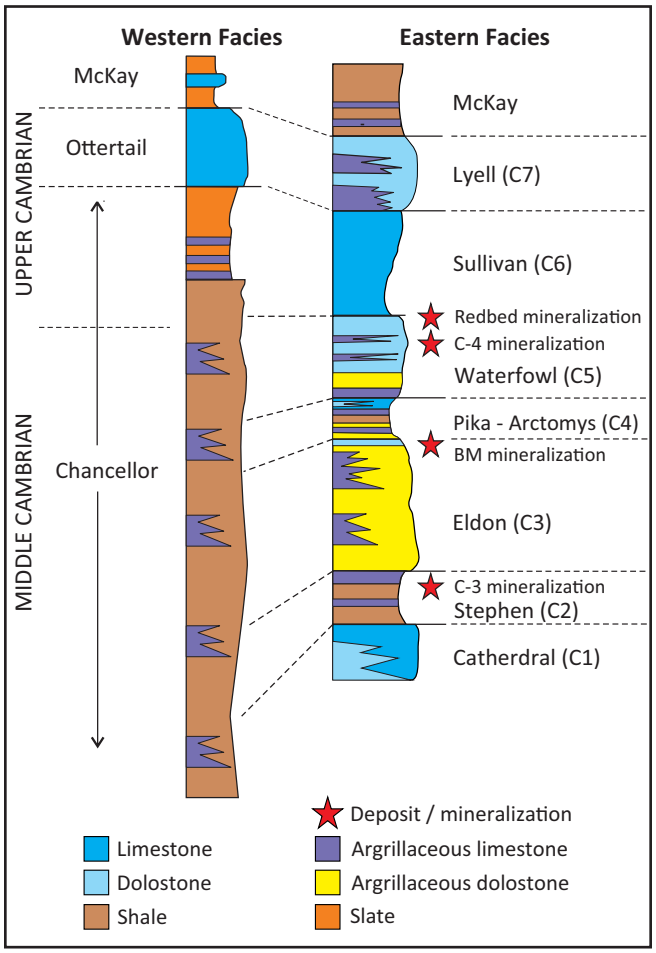

Figure 5. Stratigraphy and correlation of the Shag deposit area, British Columbia. Modified from Lenters (1982).

(Lenters, 1981). The host dolostone is sucrosic, massive, white to light grey, and contains stylolites and burrows (Lenters, 1981; Jensen, 1991). The discontinuous mineralized lenses are concentrated in sphalerite and are about 3 m thick, extending up to about 90 m along strike.

The Red Bed mineralized horizon occurs in dolostone at the top of the Middle Cambrian Waterfowl Formation (unit C5 of Bending, 1979), just below the contact with the overlying argillaceous limestone of the Sullivan Formation (unit C6 of Bending, 1979). It includes the Red Bed, Christmas, Rush, Crackle, and Pieces showings (Lenters, 1981). Stratigraphically below the strata hosting the Red Bed mineralization (Fig. 4), another dolostone unit of the Waterfowl Formation, hosts the C-4, Stripes (float), and Pad showings (Lenters, 1981). The dolostone host to the mineralization is white to light grey, sucrosic, massive, and vuggy (Lenters, 1981). Mineralization consists of small pods (≤80 cm thick and 3 m wide) that are generally higher grade than the showings in the BM horizon.

A third mineralized horizon in a thin limestone of the Stephen Formation (unit C2 of Bending, 1979) contains the C-3 showing, which occurs in a small dolomitic lens.

Munroe Deposit

Munroe is one of three Zn-Pb stratabound sulphide deposits (the others are Alpine and Boivin; collectively known as SOAB) that were discovered in the 1970s through stream sediment sampling. They are in the overturned limb of an east-verging asymmetrical anticline in the Upper Devonian Morro Member of the Palliser Formation (Fig. 6). Major westward-dipping thrust faults have positioned these Devonian rocks above Mississippian carbonate rocks and below Cambrian to Ordovician strata (Gibson, 1979a,b). Besides some geological mapping by Gibson (1979a,b) and diamond drilling in 1976 by Silver Standard Mines Ltd., very little work has been done on the Munroe, Alpine and Boivin deposits.

The host rock of the Munroe deposit is a dark grey, supratidal, muddy to silty dolostone with fenestral, medium grey to white sparry dolomite, which locally forms a texture termed ‘zebra’ dolomite. The dolostone is over- and underlain by what has been interpreted as a subtidal limestone (Gibson, 1979b). Limited field exposure precludes determination if it is the same folded bed or two different ones. The dolostone contains pale yellow to orange sphalerite (<1–10 volume %) aggregates that form bands and layers along the white sparry dolomite-filled porosity, which accentuates the zebra appearance. Sphalerite is also disseminated through the dark grey host dolostone.

Oldman Deposit

The Oldman Pb-Zn-Ag deposit, also known as Bearspaw, is located in southwestern Alberta on the eastern slope of Mount Gass. It was found by hunters in 1912 and was investigated in 1953 by the Western Canadian Collieries. Exploration work done on the property includes two adits, two short drill holes, and multiple trenches (Graf, 1998).

A dolostone in the upper part of the Late Devonian Palliser Formation hosts the stratabound deposit (Fig. 7; Holter, 1977). The Palliser Formation and overlying Mississippian strata have been thrust on to the shale and sandstone of the Cretaceous Kootenay Formation by the Lewis Thrust Fault. The host dolostone contains disseminated pyrite, sphalerite and galena, and is cut by barren and mineralized (pyrite, sphalerite, galena) white calcite (±dolomite, ankerite) veins, limonite-rich veinlets, and fault gouges parallel to and crosscutting bedding. The most spectacular feature is an intense network of irregular, flat-lying and vertically oriented, coarse-grained white calcite and grey saddle dolomite that occurs above a low-angle fault in the upper part of the Palliser Formation (Pana, 2006). Galena is the

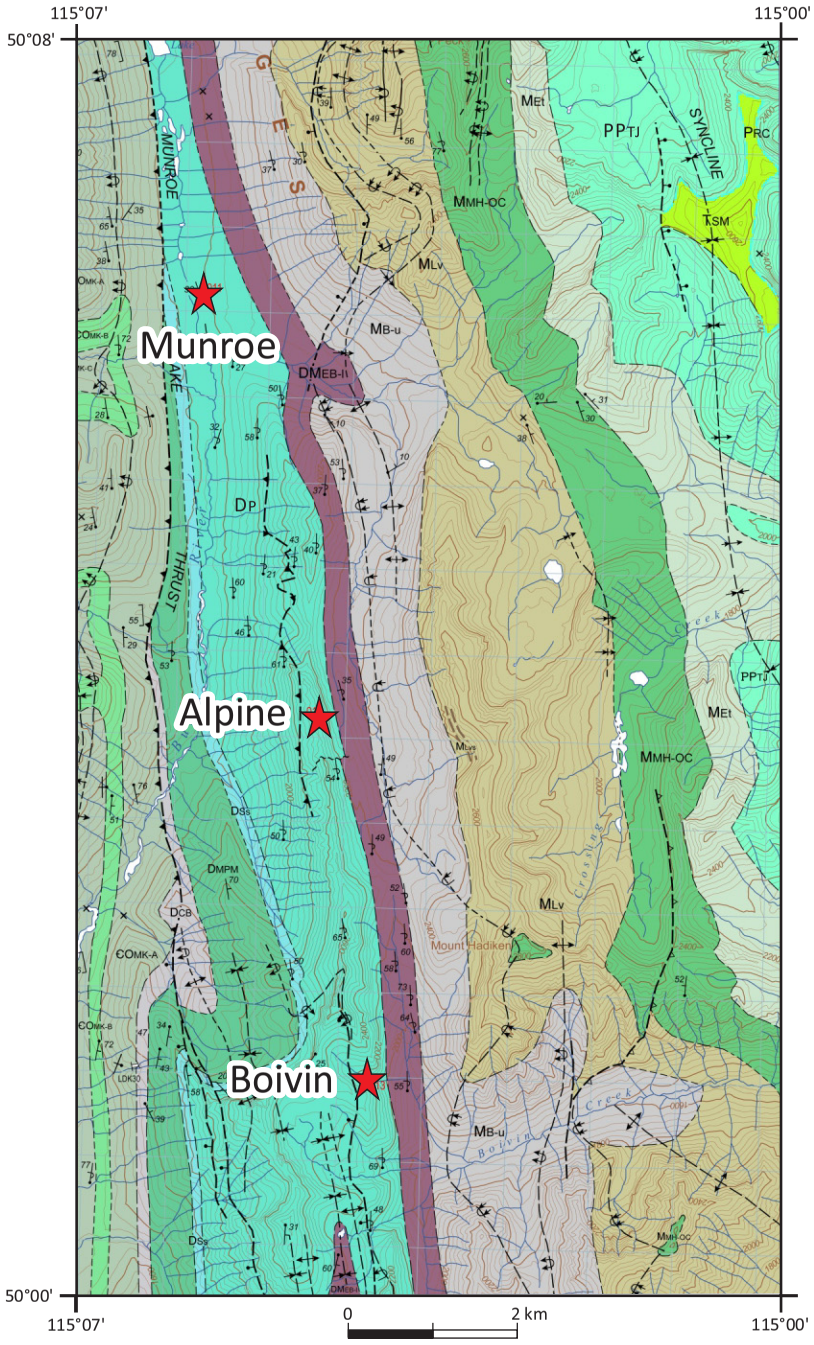

Triassic

Spray River Group

- TSM — Sulphur Mountain Formation
  Siltstone: calcareous dolomitic and soliceous

Pennsylvanian-Permian

Rocky Mountain Supergroup

- PPTJ — Tunnel Mountain and Johnston formations
  Sandstone; siltstone; occasional dolostone

Mississippian

Rundle Group

- MEt — Etherington Formation
  Lime wackestone, packstone and grainstone; dolostone; sandstone; siltstone and shale

Mount Head Formation

- MMH-OC — Opal and Carnavon members:
  Lime wackestone, packstone and grainstone; limestone, dolostone; minor shale
- MLv — Livingstone Formation
  Grainstone and packstone
- MB-u — Banff Formation (upper unit; Bourgeau facies)
  Lime wackestone and packstone; chert; lime grainstone bands

Upper Devonian-Mississippian

- DMEB-I — Exshaw and Banff (lower unit; Bourgeau facies) formations
  Shale, limy shale, lesser chert

Upper Devonian

- DP — Palliser Formation
  Limestone and dolostone, massive and mottled with well developed fenestral porosity; lesser breccia; associated Zn-Pb mineralization
- DSS — Sassenach Formation
  Siltstone and sandstone (minor shale); argillaceous limestone

Fairholme Group

- DMPM — Maligue, Perdrix and Mount Hawk formations
  Calcareous shale; argillaceous limestone; minor siltstone

Middle Devonian

- DCB — Cedared and Burnais formations
  Dolostone; mudstone; minor sandstone, limestone

Upper Cambrian-Lower Ordovician

McKay Group, upper part

- COMK-A — Unit A: Limestone-dolostone, intervals of silty and argillaceous dolostone and limestone, chert
- COMK-B — Unit B: Argillite and calcareous argillite; argillaceous limestone

Figure 6. Geology of the area surrounding the Munroe deposit and adjacent Zn-Pb deposits, Modified from McMechan and Leech (2011b).

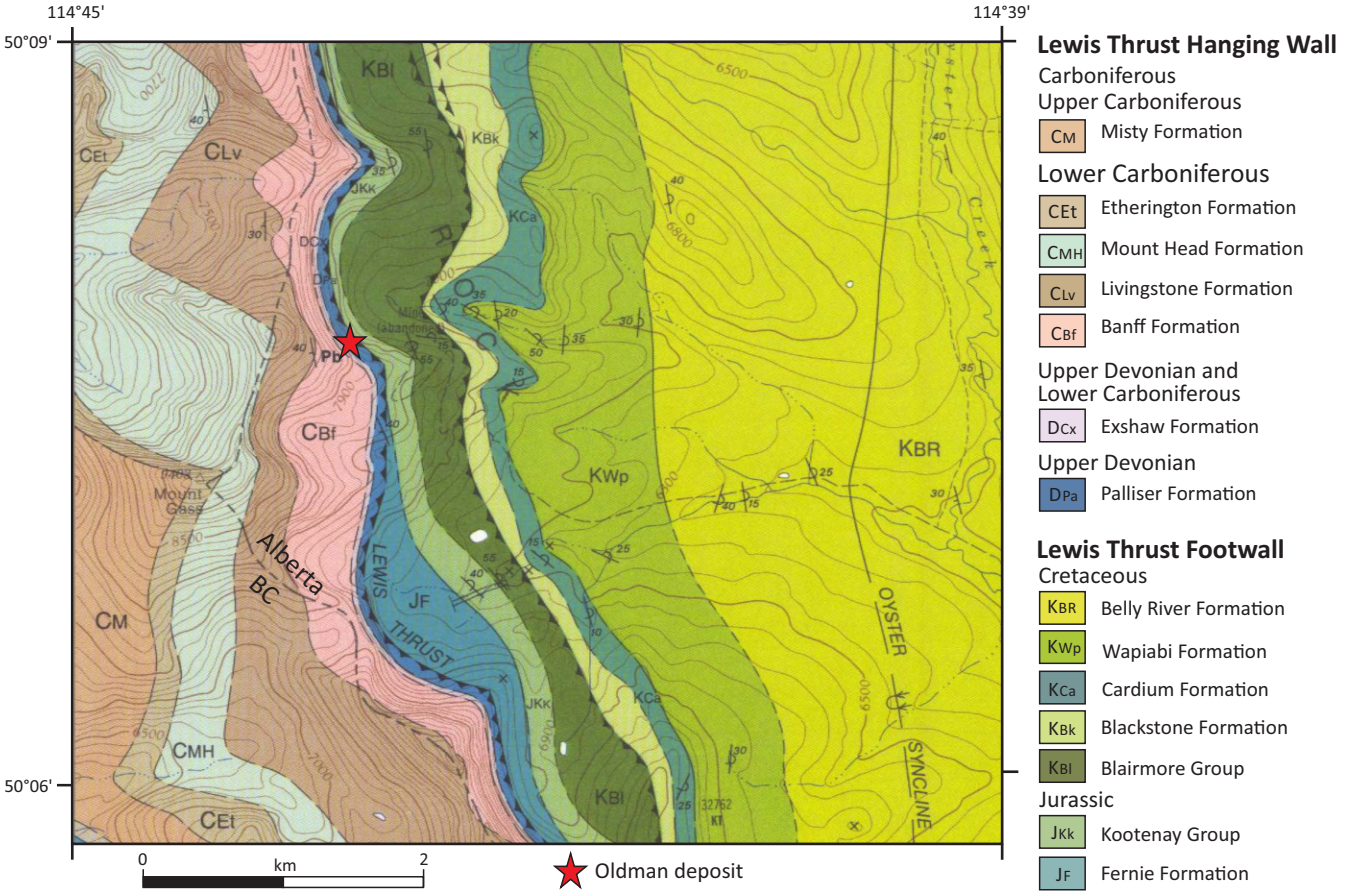

Figure 7. Geology of the Oldman deposit area, Alberta. The deposit is hosted in the Upper Devonian Palliser Formation (DPa) above the Lewis Thrust Fault. Modified from Norris (1993).

dominant sulphide mineral in the Oldman deposit and is present as disseminations in the dolomitic limestone and coarse-grained massive aggregates in calcite± dolomite veins.

Holter (1977) and Pana (2006) observed that the highest grade of mineralization was spatially associated with the intersection of thrust-and-tear faults and concluded that the mineralization was fault controlled. Salat (1988) suggested that Oldman resembles a paleokarst system that could have formed on the top of the Palliser Formation, which was then capped disconformably by the Exshaw Formation. Either or both models may be accurate, and, in general, the Oldman deposit is interpreted to be an atypical MVT deposit, i.e., an ancient paleokarst system controlled by faults and joints.

PETROGRAPHY, MINERALOGY AND PARAGENESIS OF CARBONATE-HOSTED Zn-Pb DEPOSITS

Monarch and Kicking Horse Deposits

Hand Samples

Mineralized samples from Kicking Horse are breccias with subangular to rounded, irregular-shaped, grey dolostone fragments hosted in a white sparry dolomite (± calcite) cement (Fig. 8A). The fragments are light to dark grey and range in size from a few millimetres to several centimetres in diameter. They are commonly lined with pale yellow to dark brown sphalerite (± pyrite) and some are significantly replaced by honey yellow sphalerite, minor pyrite, and galena. Sphalerite occasionally exhibits colloform textures when filling open spaces. The coarse, crystalline white sparry dolomite (± calcite) includes patches of disseminated galena (≤1 cm in diameter), fine-grained pyrite, and coarse (≤1 cm in diameter) crystalline brown sphalerite.

The mineralized sequences at Monarch are similar to those at Kicking Horse (Fig. 8B, C). However, generally they are less brecciated than at Kicking Horse and the dominant sulphide minerals are pyrite and sphalerite. White dolomite cement fills small fractures and open spaces between host dolostone fragments. Colloform sphalerite grains are crosscut by white sparry dolomite. Fine- to coarse-grained pyritohedrons form aggregates and clusters (≤5 cm in diameter) in the white sparry dolomite and, occasionally, in the host dolostone. Irregular, elongate patches of galena crosscut the white sparry dolomite cement.

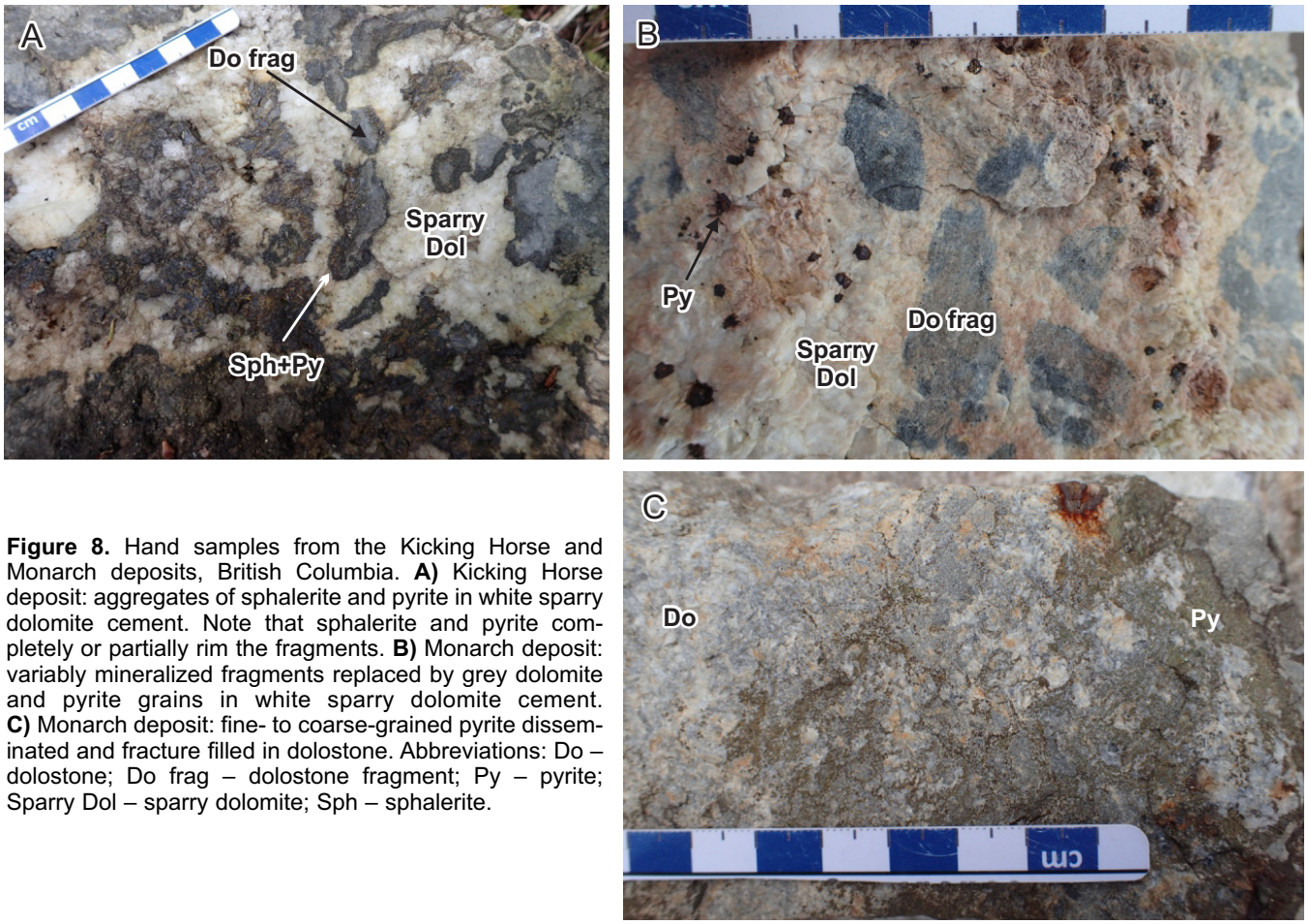

Figure 8. Hand samples from the Kicking Horse and Monarch deposits, British Columbia. **A)** Kicking Horse deposit: aggregates of sphalerite and pyrite in white sparry dolomite cement. Note that sphalerite and pyrite completely or partially rim the fragments. **B)** Monarch deposit: variably mineralized fragments replaced by grey dolomite and pyrite grains in white sparry dolomite cement. **C)** Monarch deposit: fine- to coarse-grained pyrite disseminated and fracture filled in dolostone. Abbreviations: Do – dolostone; Do frag – dolostone fragment; Py – pyrite; Sparry Dol – sparry dolomite; Sph – sphalerite.

Mineralogy and Paragenesis

The petrographic textures and relationships observed in the samples from the Monarch and Kicking Horse deposits establish a paragenetic sequence of minerals (Fig. 9). The host rock to Monarch and Kicking Horse is a dark grey, fine-grained (0.02–0.15 mm in diameter) dolostone (≤60 volume %) that contains remnant allochems and inclusions of organic material. The dolostone is replaced by light grey, anhedral, fine- to medium-grained (0.01–0.2 mm in diameter) crystalline dolomite (10–40 volume %; Fig. 10A). Vandeginste et al. (2007) described the dark grey dolostone as fabric-preserving that is partially to completely replaced by fabric-destructive light grey dolomite. Both are fractured, brecciated, and form the fragments of the mineralized breccias. Fragments are enclosed in a matrix of dark grey dolomite (i.e. the 'grey breccia' of Ney, 1954) that contains insoluble material or in a matrix of white sparry dolomite (i.e. the 'white breccia' of Ney, 1954).

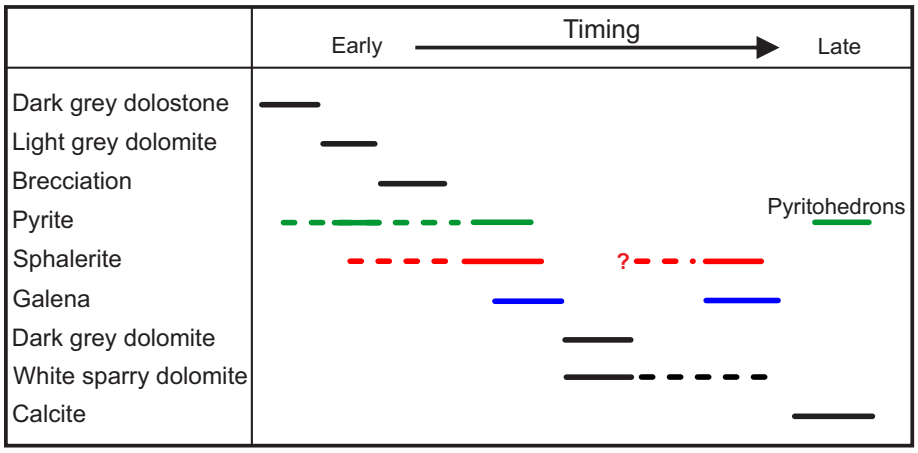

Figure 9. Simplified paragenetic sequence of minerals in samples from the Monarch and Kicking Horse deposits, British Columbia, indicating several generations of dolomite, pyrite, sphalerite, and galena. Dashed lines and the interrogation mark refer to uncertainty in the timing of the precipitation of the minerals.

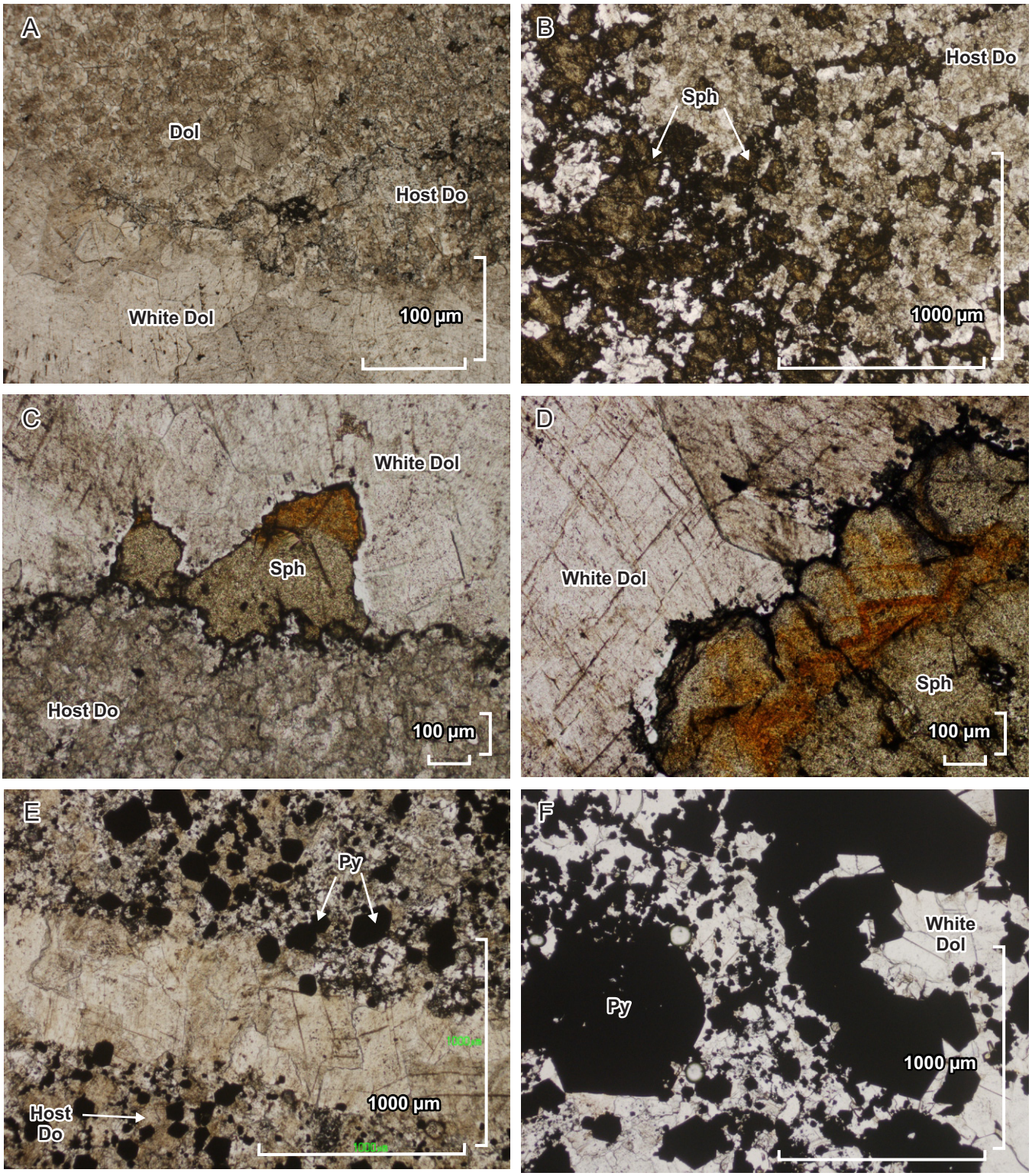

Figure 10. Photomicrographs showing textures in samples from the Kicking Horse and Monarch deposits, British Columbia. **A)** Three phases of dolomite: dark grey host dolostone (oldest), recrystallized grey dolomite, and white sparry dolomite (youngest); plane polarized light (PPL). **B)** Intergranular brown sphalerite in the host dolostone; PPL. **C)** Sphalerite exhibiting colour zonation with 'snow-on-the-roof' texture forming along a fragment of the host dolostone; PPL. **D)** Colloform sphalerite exhibiting colour zonation adjacent to white sparry dolomite; PPL. **E)** White dolomite vein crosscutting the host dolostone, which is rich in recrystallized pyrite; PPL. **F)** Pentagonal dodecahedrons of pyrite (pyritohedrons) associated with white dolomite; PPL. Abbreviations: Dol – recrystallized dolomite; Host Do – host dolostone; Py – pyrite; Sph – sphalerite; White Dol - white sparry dolomite.

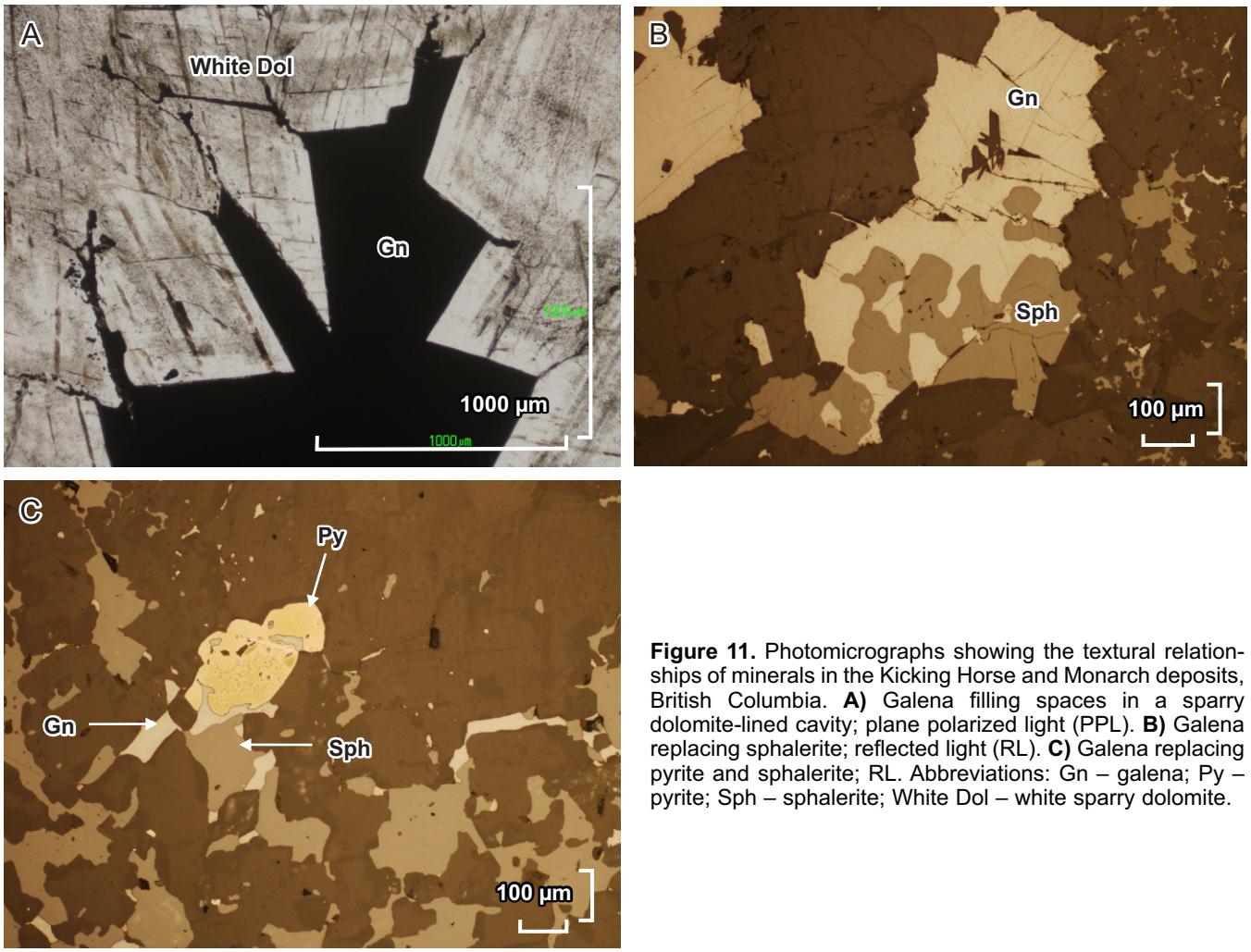

Figure 11. Photomicrographs showing the textural relationships of minerals in the Kicking Horse and Monarch deposits, British Columbia. **A)** Galena filling spaces in a sparry dolomite-lined cavity; plane polarized light (PPL). **B)** Galena replacing sphalerite; reflected light (RL). **C)** Galena replacing pyrite and sphalerite; RL. Abbreviations: Gn – galena; Py – pyrite; Sph – sphalerite; White Dol – white sparry dolomite.

Overall, sphalerite is more abundant in our Kicking Horse samples, with an approximate volume of 15 to 20% compared to 5 to 10% in the Monarch samples. An early phase of very fine-grained (0.04–0.1 mm in diameter), dark brown sphalerite is disseminated in both the host dolostone and the light grey dolomite, but seems preferentially associated with the host dolostone. A later phase of slightly coarser (0.1–0.4 mm in diameter), granular, honey yellow to brown sphalerite replaces the host dolostone (Fig. 10B), occasionally forming aggregates and occurring along the perimeter of fragments. Coarse-grained (0.5–1 mm in diameter) sphalerite fills vugs and fractures, where it commonly exhibits crustification banding with colloform textures and colour zonation from light brown to red (Fig. 10C, D).

Pyrite (trace to 25 volume %) is present in multiple phases. Early very fine-grained (<0.005 mm in diameter), rounded pyrite that resembles framboids is disseminated in the host dolostone. Later fine-grained (0.005–0.02 mm in diameter), subrounded pyrite is closely associated and intergrown with sphalerite. Coarser (0.05–0.2 mm in diameter) recrystallized pyrite overprints the host dolostone, grey dolomite, and sphalerite (Fig. 10E). Late pyritohedrons (0.8–2.5 mm in diameter) are disseminated in the white sparry dolomite cement of the breccias and veins, and line the walls of cavities (Fig. 10F).

Galena (5–15 volume %) forms irregular-shaped masses (≤1.6 mm in diameter) that fill open spaces and fractures (Fig. 11A) and replace sphalerite (Fig. 11B), pyrite (Fig. 11C), and the white dolomite. Fine-grained (0.02–0.2 mm in diameter) galena makes up less than 2% of the samples and is disseminated in the white sparry dolomite.

White sparry dolomite fills cavities and fractures, and forms veins with euhedral, crystalline, coarse-grained crystals (0.8–1 mm in diameter; Fig. 10C, D, E) that crosscut fragments and the matrix of the ‘grey breccia’. This dolomite is barren or mineralized by crystalline, subhedral to euhedral, medium- to coarse-grained (0.8–15 mm in diameter) sphalerite, fractured colloform sphalerite, and other sulphide minerals.

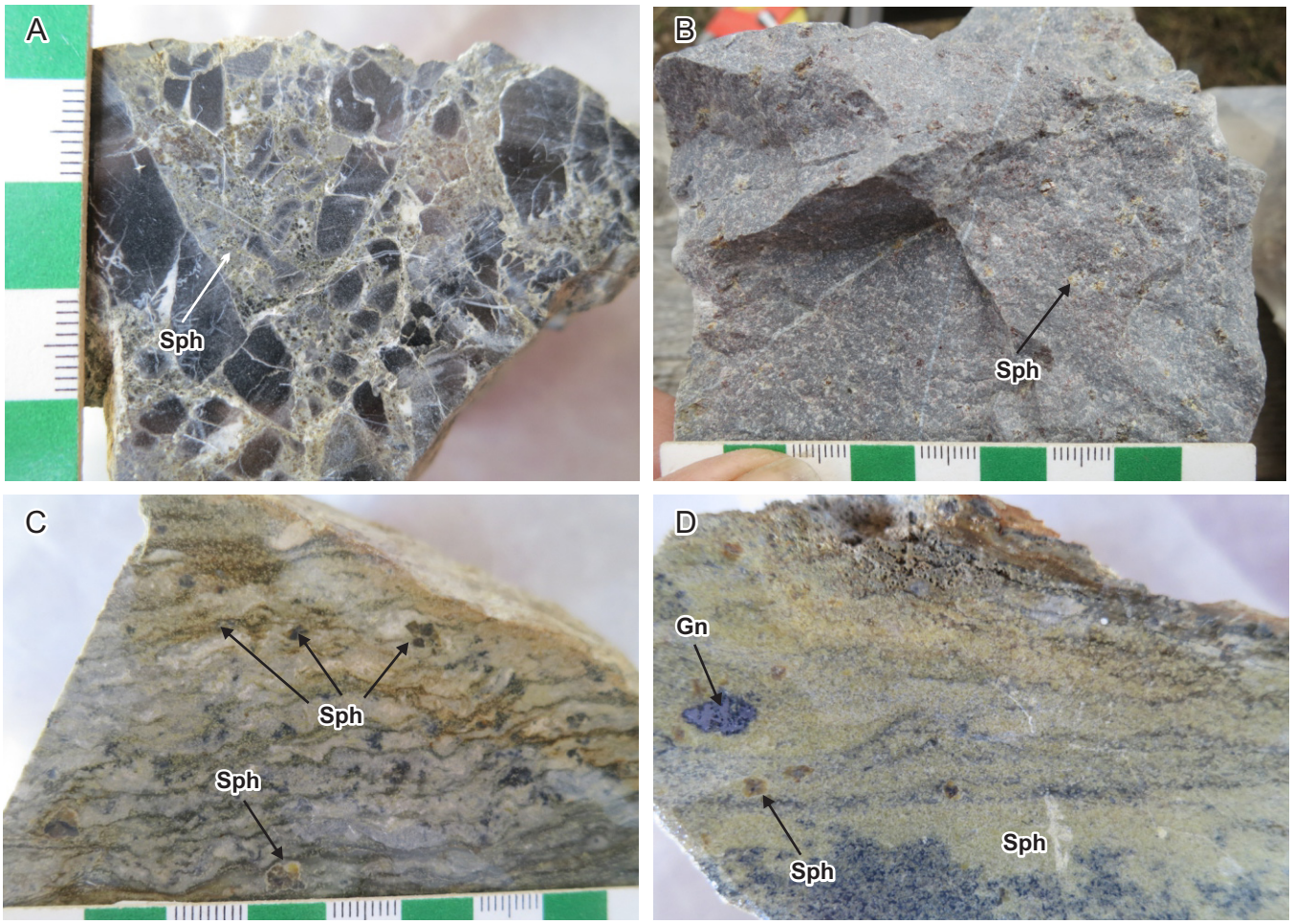

Figure 12. Hand samples from the C-3, BM, and C-4 showings, Shag deposit, British Columbia. **A)** C-3 showing: angular to subrounded dark dolostone fragments in a matrix of dolomite (±calcite), yellow sphalerite, and pyrite. Non-mineralized veinlets of white sparry dolomite crosscut all phases. **B)** BM showing: fine-grained pale grey dolostone containing disseminated vugs (<3 mm in diameter) filled by white sparry dolomite and sphalerite. **C)** C-4 showing: dolostone with moderate replacement by lenses of yellow sphalerite and white to pale grey sparry dolomite; note coarse aggregates of sphalerite crystals. **D)** C-4 showing: sample has intense replacement of the dolostone by yellowish granular sphalerite and white sparry dolomite; large euhedral crystals of pale yellow sphalerite (up to approximately 3 mm in diameter) and clots of galena (approximately 0.8 mm long). Abbreviations: Gn – galena; Sph – sphalerite.

Shag Deposit

Hand Samples

Samples from the Shag deposit come from the C-3, BM, C-4, and Red Bed showings. Although they have similar mineralogy (sulphides: sphalerite, galena, and pyrite; gangue: dolomite and quartz), they have variable textures (disseminations, replacement, and veins) and sulphide content.

C-3 showing (Fig. 12A): The sample from the C-3 showing is a dolostone breccia containing dark grey, angular to subrounded fragments ranging from 0.5 mm to a few cm across in a matrix of dolomite (± calcite), yellow sphalerite, and pyrite. Non-mineralized veinlets of white sparry dolomite pervasively crosscut the sample. Although no galena was observed in this sample, it has been reported as irregular, elongate inclusions (averaging 0.02–0.03 mm long) in sphalerite (Graf, 1998).

BM showing (Fig. 12B): Mineralized samples from the BM showing consist of massive, fine-grained, pale grey dolostone containing white sparry dolomite filled vugs and fractures. Disseminated yellow to reddish sphalerite crystals are mainly concentrated along the rim and edge of the white sparry dolomite-filled vugs and fractures. The dolostone is crosscut by non-mineralized white dolomite veinlets. One sample (not shown in Fig. 12) is a darker grey dolostone with a layered texture caused by alignment of voids filled by white sparry dolomite, and lenses or patches of pale grey altered dolostone. Small grains of disseminated sphalerite replace the dark grey dolostone and are preferentially associated with the pale grey dolomite patches.

C-4 showing (Fig. 12C, D): Samples from the C-4 showing have intense replacement of the host dolostone by yellowish granular sphalerite and white to pale grey sparry dolomite. Both form wispy lenses that

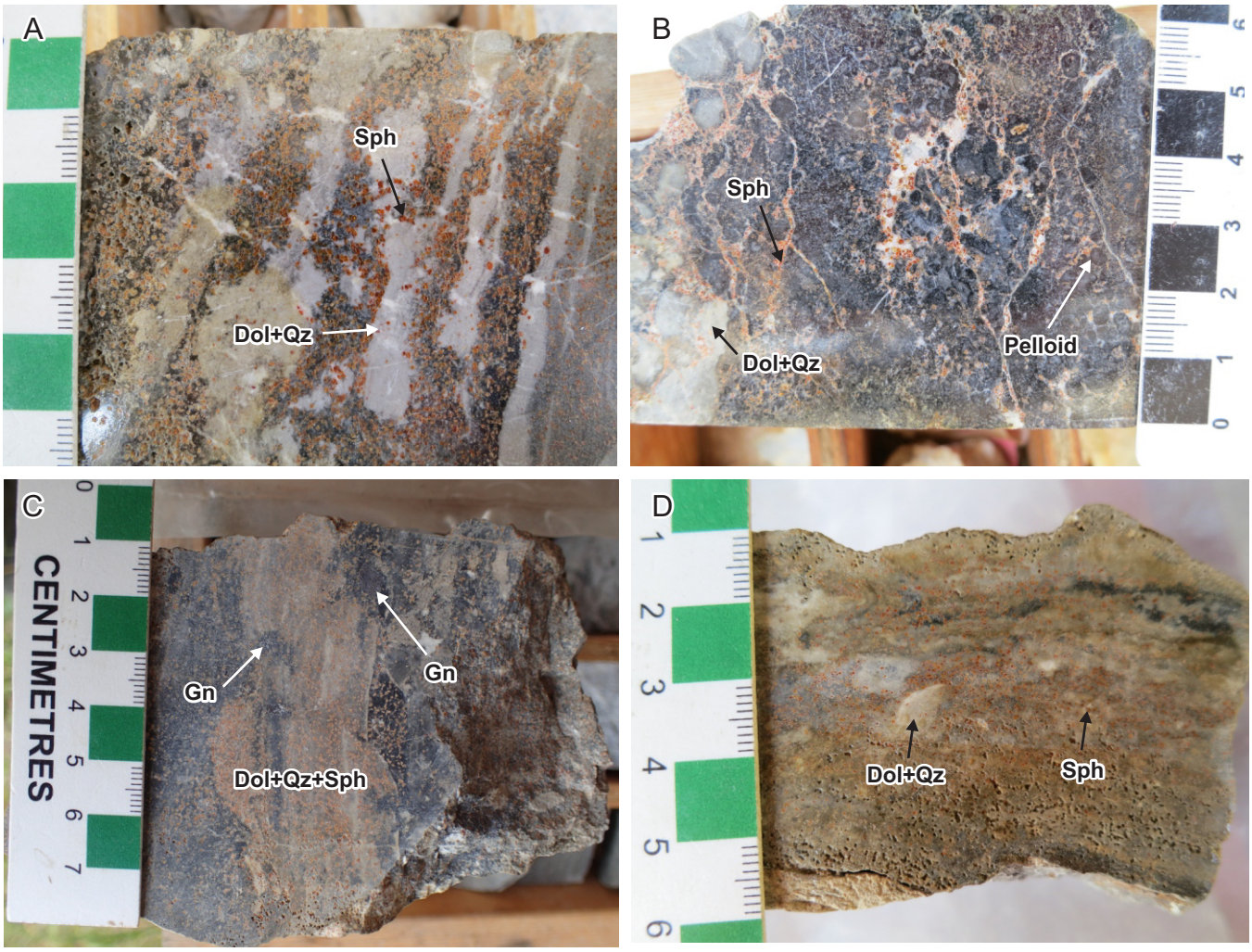

Figure 13. Hand samples from the Red Bed showing, Shag deposit, British Columbia. **A)** Alternating bands of white dolomite-quartz and fine-grained dark dolostone rich in disseminated red sphalerite. **B)** Dark grey dolostone rich in pelloids or ooids replace by an aggregate of white sparry dolomite (±quartz) and crosscut by a network of white sparry dolomite (±quartz) and red sphalerite-bearing veinlets. **C)** Broadly banded and layered sample showing replacement of the dark grey dolostone by patches and layers of fine-grained quartz, dolomite, and red sphalerite. Coarse-grained galena crystals and stringers are present. **D)** Dolostone with intense replacement by an assemblage of quartz, dolomite, and red sphalerite. Abbreviations: Dol+Qz – fine-grained mixture of dolomite and quartz; Dol+Qz+Sph – fine-grained mixture of dolomite, quartz and sphalerite; Gn – galena; Sph – sphalerite.

give a broad layered appearance to the dolostone. Large euhedral crystals of pale yellow sphalerite (≤1 cm in diameter) and clots of galena (~0.8 mm long) are locally disseminated in the mineralized portions of the samples.

Red Bed showing (Fig. 13A, B, C, D): Samples from the Red Bed showing consist of broadly irregularly banded and layered dolostone, which is characterized by an abundance of fine-grained quartz and distinct orange to reddish sphalerite (≤60 volume %). The irregular bands are millimetre- to centimetre-thick, variably mineralized, and consist of fine-grained dark dolostone alternating with a mixture of pale grey dolostone and quartz. One sample, Shag 8 (not shown in Fig. 13), is a dolostone rich in allochems (peloids or ooids) that is crosscut by veinlets and patches of coarse-grained dolomite, sphalerite, and quartz. Allochems are rarely seen in the other samples.

Mineralogy and Paragenesis

C-3 showing: The petrographic textures and relationships observed in a sample from the C-3 showing establish a paragenetic sequence of minerals (Fig. 14). The host dolostone fragments are composed of fine-grained, equant, and recrystallized dolomite grains (0.01–0.1 mm in diameter). The fragments contain disseminated, very fine-grained (0.0005–0.05 mm in diameter), subhedral and rounded pyrite (0.5–3 volume %; Fig. 15A), and occasional disseminated grains of sphalerite (0.0005–0.01 mm in diameter). The matrix enclosing the fragments consists of recrystallized, fine-grained (0.2–0.6 mm in diameter), crystalline dolomite

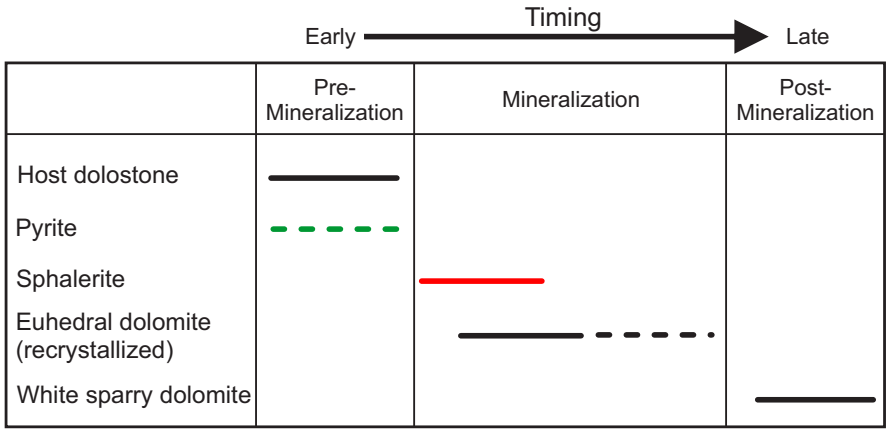

Figure 14. Simplified paragenetic sequence of minerals in samples from the C-3 showing, Shag deposit, British Columbia. Dashed lines refer to uncertainty in the precipitation timing of minerals.

(15 volume %) and medium-grained (0.2–0.6 mm in diameter) sphalerite (25 volume %; Fig. 15B). This crystalline dolomite occasionally overprints the sphalerite grains and forms veinlets that crosscut the host dolostone fragments. The sphalerite is typically honey yellow to light brown, granular, and has irregular boundaries due to alteration to smithsonite ($ZnCO_3$). The sphalerite frequently forms elongated aggregates

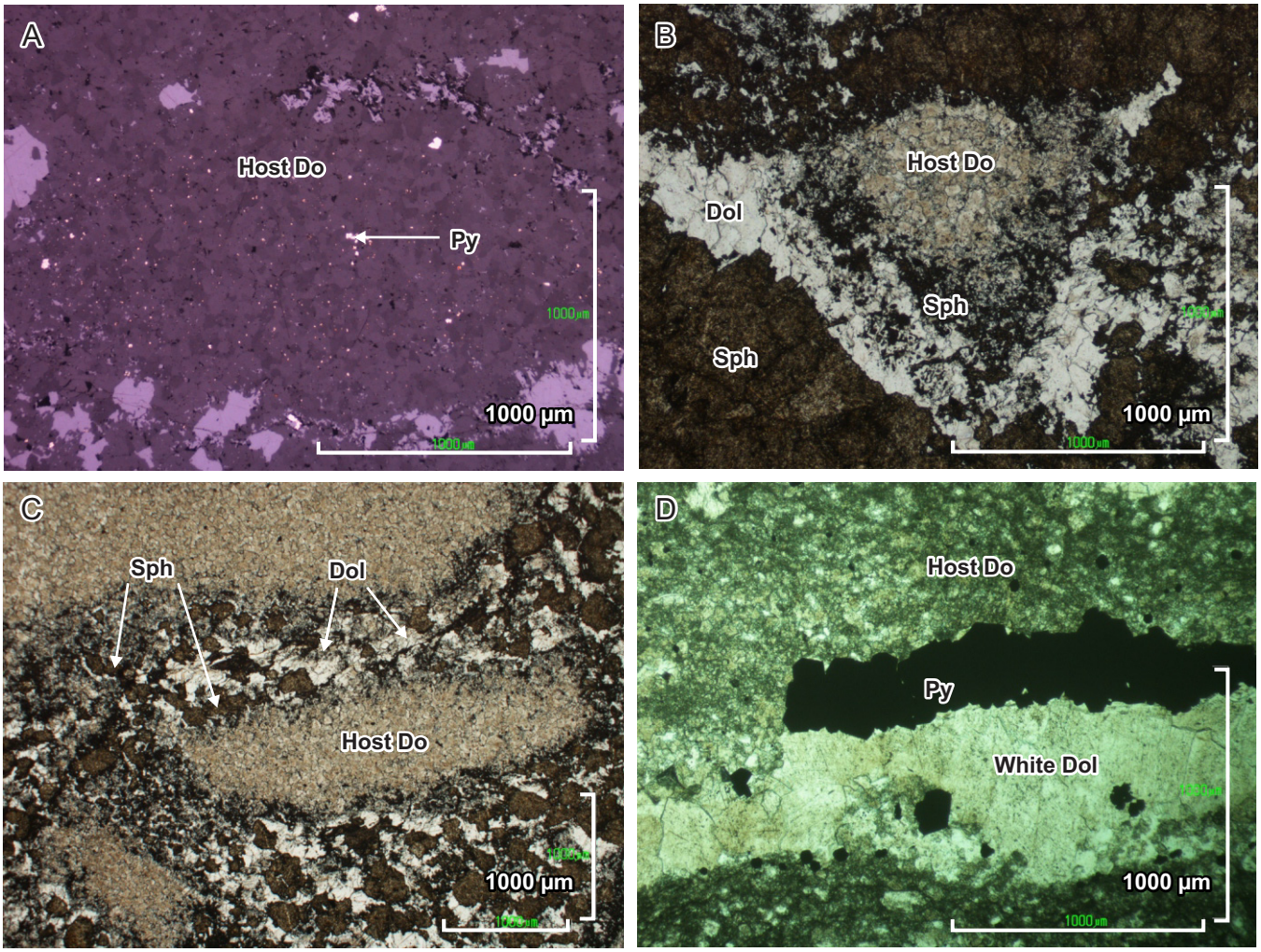

Figure 15. Photomicrographs showing the textural relationships of mineral phases in the C-3 and BM showings, Shag deposit, British Columbia. **A)** C-3 showing: disseminated pyrite in the host dolostone; reflected light (RL). **B)** C-3 showing: fragment of host dolostone lined with fine-grained sphalerite adjacent to coarse-grained sphalerite and a crystalline dolomite veinlet; plane polarized light (PPL). **C)** C-3 showing: fragment of host dolostone, replaced by sphalerite along boundaries; PPL. **D)** BM showing: elongate aggregate of pyrite in contact with host dolostone and white sparry dolomite. Abbreviations: Dol – dolomite; Host Do – host dolostone, Py – pyrite; Sph – sphalerite; White Dol – white sparry dolomite.

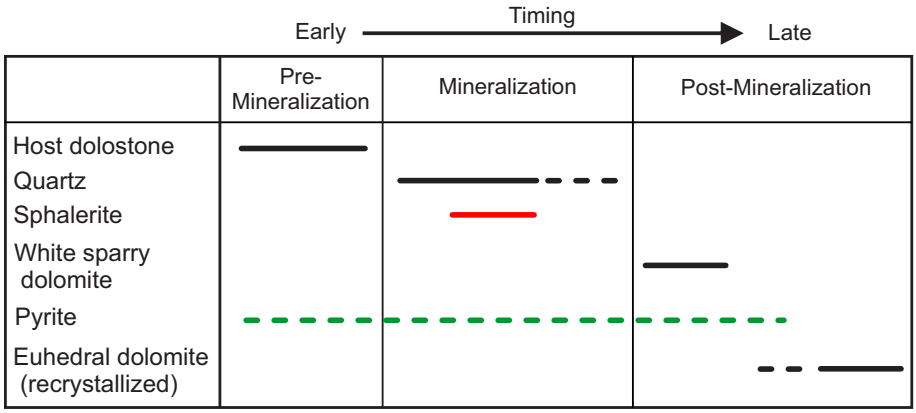

Figure 16. Simplified paragenetic sequence of minerals in samples from the BM showing, Shag deposit, British Columbia. Dashed lines refer to uncertainty in the precipitation timing of minerals.

of grains in the crystalline dolomite that cements the dolostone fragments. The fragments are commonly lined with fine-grained (<0.01 mm in diameter) sphalerite (Fig. 15C). The sphalerite and crystalline dolomite are likely contemporaneous, although their relationship is not always clear because recrystallization has partially obscured original textures. White sparry dolomite (15 volume %) fills spaces, such as fractures and vugs. It is coarse-grained (0.2–0.8 mm in diameter) and non-mineralized, but occasionally contains fractured sphalerite and pyrite grains.

BM showing: The petrographic textures and relationships observed in the samples from the BM showing establish a paragenetic sequence of minerals (Fig. 16). The host rock to the BM showing is a dark dolostone with fine-grained (0.005–0.2 mm in diameter) subhedral dolomite crystals that contain fluid and opaque inclusions measuring <0.005 mm across, which give the dolomite a cloudy appearance. The dolostone contains stylolites and remnant allochems preserved from its limestone precursor. Fine- to medium-grained (0.05–0.3 mm in diameter), sub-rounded quartz (15–30 volume %) replaces the host dolostone, and very fine-grained pyrite is disseminated through the dolostone. Sphalerite (1–5 volume %) occurs as fine- to medium-grained (0.1–0.8 mm in diameter), irregular-shaped crystals that fill open spaces (vugs and fractures) and locally replace the host dolostone. This sphalerite varies in colour from yellow to red, and some grains show a colour zonation in transmitted light. The sphalerite that replaces the dolostone is fine-grained and intergrown with dolomite and quartz, and is locally replaced by quartz. Sphalerite that fills open spaces and fractures is associated with sparry dolomite and quartz. In one sample, cockade sphalerite (3 volume %), accompanied by quartz and dolomite, forms small veinlets that are cut by vugs filled by sphalerite (0.1–0.4 mm in diameter), quartz, and dolomite. Sparry, coarse-grained (0.6–1 mm in diameter) white dolomite (15–20 volume %) fills fractures and spaces, forming elongate wispy lenses. Quartz commonly surrounds and is intergrown with this phase of dolomite. Except for the occasional pyrite grain, this dolomite is not mineralized. Fine (0.01–0.1 mm in diameter), subhedral to euhedral grains of pyrite are disseminated throughout the host dolostone, and intermittently in the white sparry dolomite (1–2 volume %). Pyrite also forms elongate aggregates (≤4 mm) of euhedral crystals associated with white sparry dolomite (Fig. 15D). Microcrystalline to fine (<0.1 mm in diameter), euhedral dolomite grains are ubiquitously scattered throughout the samples, overprinting all mineral phases. They are the product of recrystallization.

C-4 showing: The paragenetic sequence of minerals in samples from the C-4 showing is presented in Figure 17. The host dolostone of the C-4 showing is difficult to see in our samples because of intense replacement. Remnants are wispy lenses of dark grey dolostone

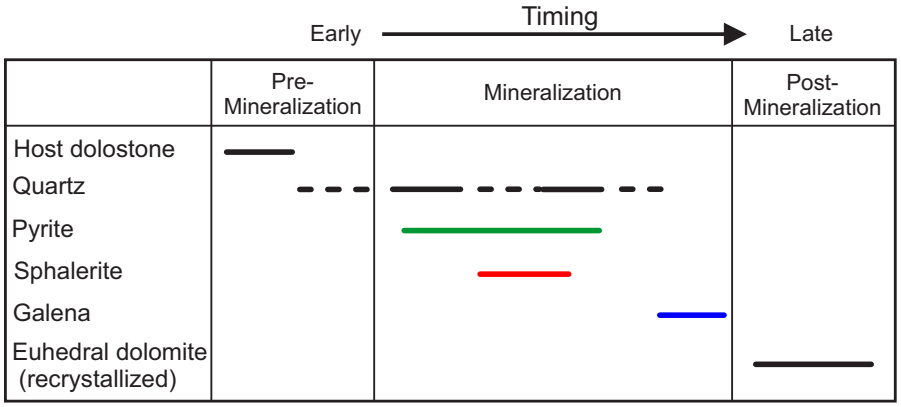

Figure 17. Simplified paragenetic sequence of minerals in samples from the C-4 showing, Shag deposit, British Columbia. Dashed lines refer to uncertainty in the precipitation timing of minerals.

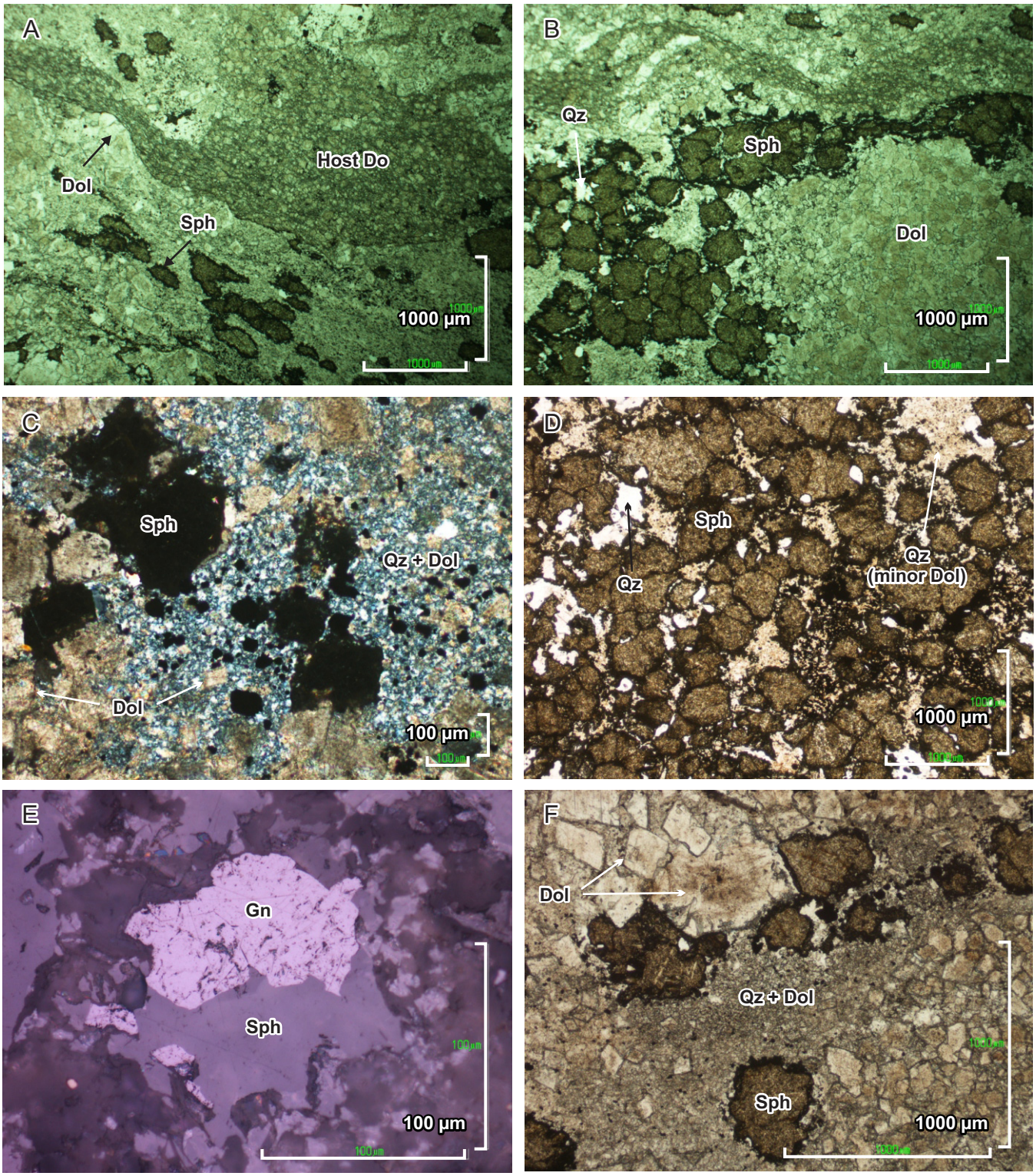

Figure 18. Photomicrographs showing the textural relationships of mineral phases in the C-4 showing, Shag deposit, British Columbia. **A)** Least replaced sample showing remnant wispy lens of dolostone composed of microcrystalline to fine-grained, euhedral to subhedral and occasionally rhombic dolomite crystals; plane polarized light (PPL). **B)** Least replaced sample showing remnant wispy lens of dolostone and irregular band of granular sphalerite in a matrix of dolomite and minor quartz; PPL. **C)** Moderately replaced sample with coarse-grained sphalerite in a matrix of quartz-dolomite; crossed-polarized light. **D)** Intense replacement by aggregates of equant, granular sphalerite in a matrix of fine-grained dolomite and quartz, with minor pyrite and galena (black); PPL. **E)** Galena associated with sphalerite in a quartz-dolomite assemblage; RL. **F)** Equant, euhedral dolomite crystals overprinting a fine-grained quartz-dolomite assemblage; PPL. Abbreviations: Dol – dolomite; Host Do – host dolostone, Gn – galena, Py – pyrite, Qz + Dol – quartz-dolomite matrix, Sph – sphalerite.

composed of microcrystalline to fine-grained, euhedral to subhedral and occasionally rhombic dolomite crystals (Fig. 18A). Lesser replaced samples (e.g. Fig. 12C) consist of wavy and irregular bands and lenses composed dominantly of equant and euhedral to subhedral dolomite and minor calcite (0.02–0.2 mm in diameter), and less abundant lenses and patches of microcrystalline to fine-grained quartz and minor dolomite (Fig. 18B, C). The quartz-dolomite zones preferentially host sphalerite, galena, and pyrite. The most replaced samples (e.g. Fig. 12D) consist of massive aggregates of granular sphalerite that forms broad bands or patches in a matrix of microcrystalline quartz, dolomite, and minor pyrite and galena (Fig. 18D). There are two generations of quartz present in the samples from the C-4 showing. The first generation is microcrystalline (10–30 volume %) and is locally replaced and intergrown with sphalerite. The second generation (5–15 volume %) consists of irregular-shaped, fine- to medium-grained, transparent crystals (0.2–0.5 mm in diameter) and crosscuts or is intergrown with sphalerite. Sphalerite (15–50 volume %) occurs as equant, granular, medium-sized (0.25 mm in diameter), pale brown grains. It forms clusters or bands (Fig. 18D) and replaces the host dolostone. Alteration of the sphalerite grain boundaries to smithsonite ($ZnCO_3$) contributes to their irregular shapes. Single large grains (<3 mm in diameter) and aggregates (2–7 mm in diameter) of dark brown sphalerite are observed in the quartz-dolomite assemblage. They are the recrystallized products of the earlier, finer-grained sphalerite. Pyrite is a minor component (0.5–3 volume %) of the samples studied from the C-4 showing. It is fine-grained, subhedral, and disseminated throughout the quartz-dolomite assemblage. It forms clusters 0.4 to 2 mm in size of fine (0.1–0.2 mm in diameter), rounded grains that locally replace sphalerite. Fine-grained pyrite (0.02–0.06 mm in diameter) is also present as inclusions within sphalerite. This suggests that pyrite occurred before, during, and after sphalerite mineralization. Galena (trace to 5 volume %) is concentrated in the quartz-dolomite zones where it occurs as interstitial, irregular-shaped grains (0.01–0.03 mm in diameter) and is locally associated with sphalerite and pyrite. Galena in contact with dolomite has an altered, discontinuous rim of cerussite ($PbCO_3$), which is absent when in contact with sphalerite (Fig. 18E). Recrystallized dolomite with equant, euhedral, transparent grains is disseminated throughout the samples and is the last phase to crystallize (Fig. 18F).

Red Bed showing: The paragenetic sequence of minerals in samples from the Red Bed showing is presented in Figure 19. The mineralized samples from the Red Bed showing consist of irregular, variably altered and mineralized bands and layers composed of an assemblage of quartz (≤60 volume %), sphalerite (15–20 volume %), and lesser dolomite (10–20 volume %), galena (<3 volume %), and pyrite (<2 volume %). The host rock (e.g. Fig. 13B) is a fine-grained (0.1–0.2 mm in diameter) dolostone composed of equant dolomite grains 0.05 to 0.1 mm in diameter and minor microcrystalline quartz; occasional remnant ooids are visible (Fig. 20A). Brown sphalerite is present as disseminated, irregular-shaped grains that are interstitial to the dolomite. Quartz is abundant in the samples where it forms aggregates of microcrystalline to fine-grained (0.04–0.2 mm in diameter), non-oriented, and interlocking grains with minor dolomite. Some of the coarser transparent grains have subhedral to euhedral prismatic boundaries. Quartz also crosscuts and replaces sphalerite and dolomite crystals. Sphalerite is granular, medium-grained (0.5–1 mm in diameter), and commonly shows colourless to orange zonation in plane-polarized light (Fig. 20B). It fills open spaces and replaces the host dolostone. The grains are irregular-shaped due to alteration to smithsonite along the grain boundaries, and from taking the shape of open spaces and replaced minerals. Dolomite forms fine (< 0.1 mm in diameter), anhedral to subhedral individual grains disseminated in the quartz-rich bands and layers, and aggregates of grains forming patches and lenses (Fig. 20C). In all samples, euhedral rhombic dolomite crystals (≤100 µm in diameter) are disseminated throughout and overprint all mineral phases. They represent the

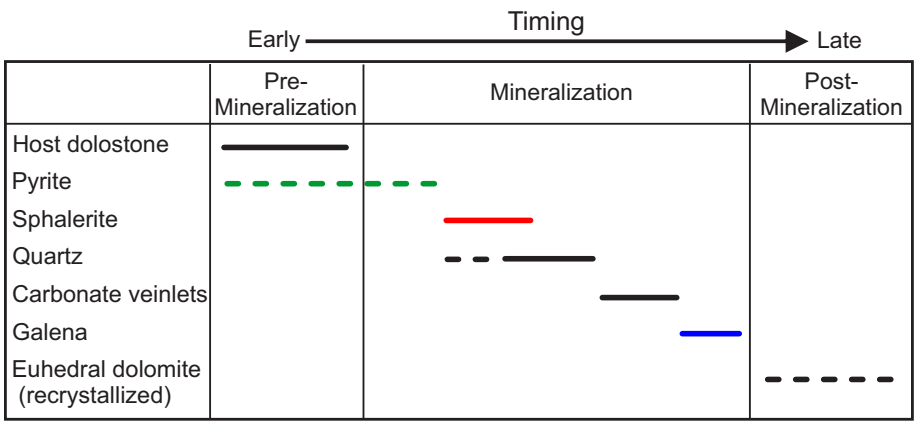

Figure 19. Simplified paragenetic sequence of minerals in samples from the Red Bed showing, Shag deposit, British Columbia. Dashed lines refer to uncertainty in the precipitation timing of minerals.

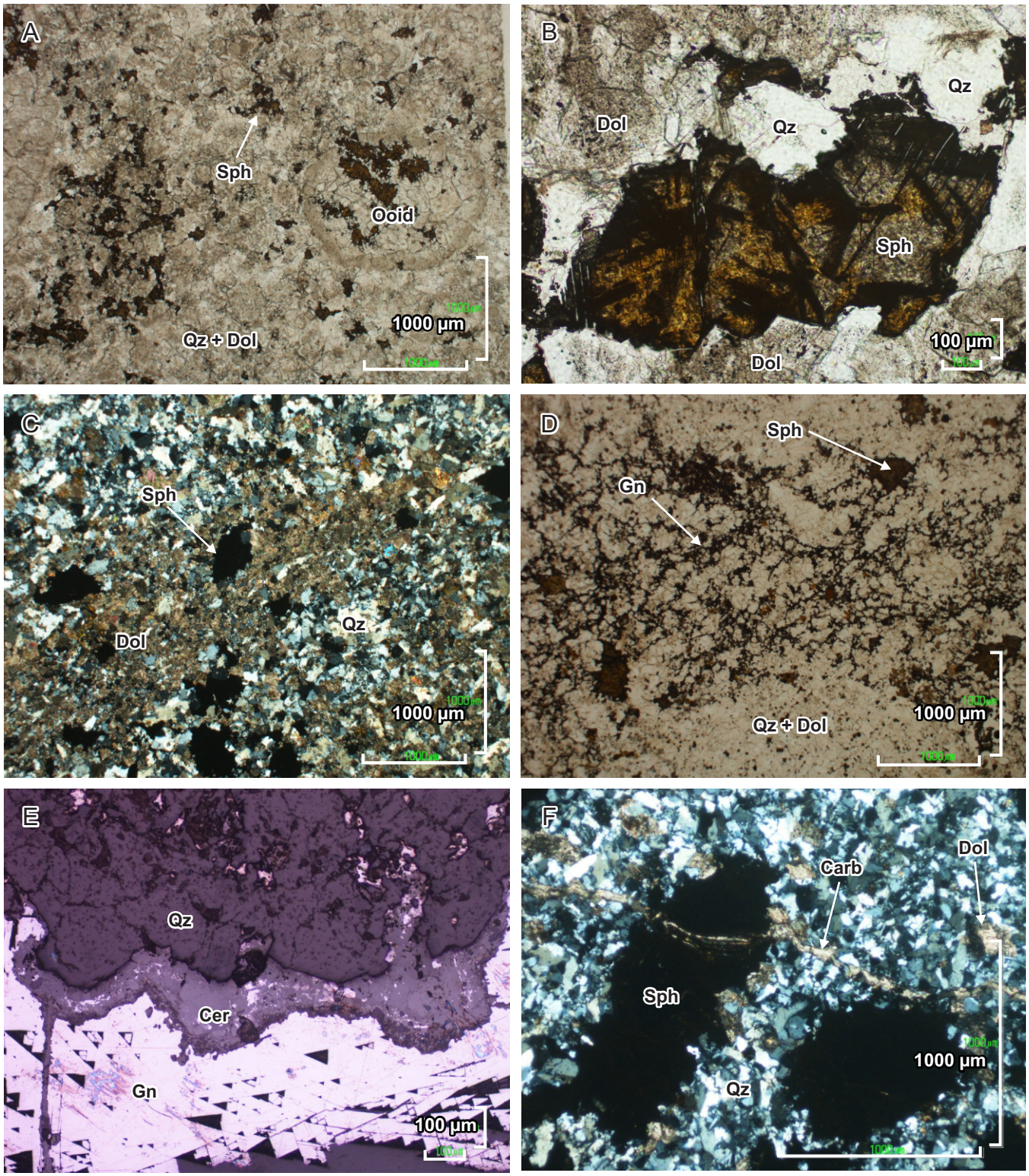

Figure 20. Photomicrographs showing the textural relationships of mineral phases of the Red Bed showing, Shag deposit, British Columbia. A) Dolomite-quartz matrix with interstitial sphalerite. Note the remnant ooid; plane polarized light (PPL). **B)** Sphalerite showing colour zonation in the quartz and dolomite matrix; note the alteration around and within sphalerite; PPL. **C)** Fine-grained dolomite-rich lens (minor quartz) surrounded by a quartz-rich matrix with minor dolomite; crossed-polarized light (XPL). **D)** Quartz-dolomite matrix with interstitial galena and sphalerite; PPL. **E)** Galena altered to cerussite along the perimeter; reflected light. **F)** Fine-grained carbonate veinlet cuts a sphalerite grain and the quartz-rich matrix; XPL. Abbreviations: Carb – carbonates; Cer – cerussite; Dol – recrystallized dolomite; Gn – galena; Qz – quartz; Qz + Dol – quartz-dolomite assemblage; Sph – sphalerite.

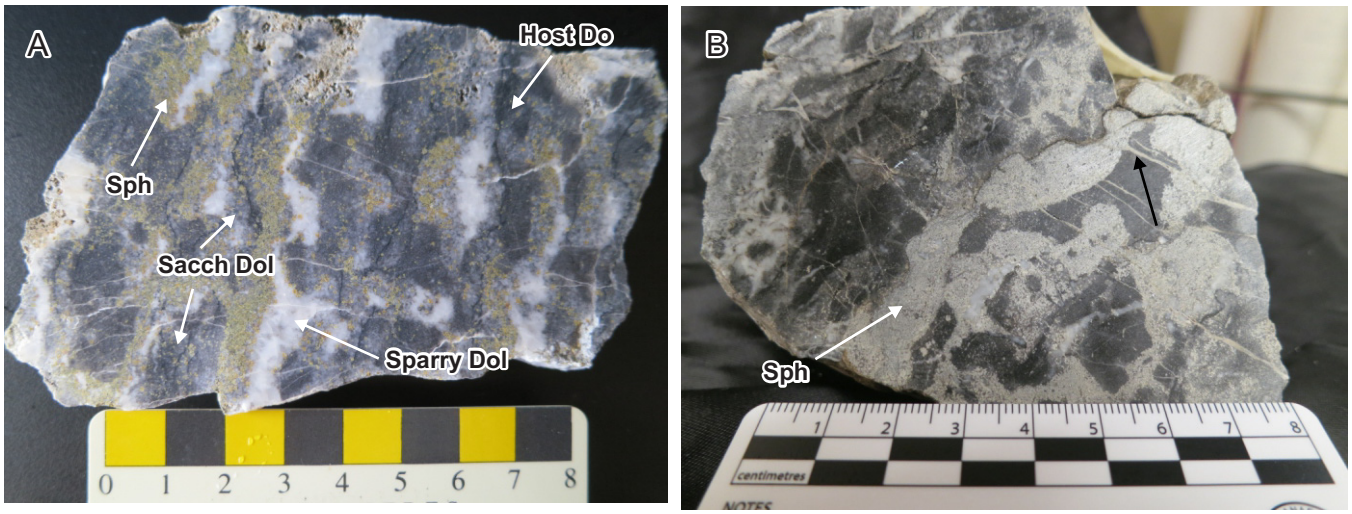

Figure 21. Hand samples from the Munroe deposit, British Columbia. **A)** Zebra-like texture created by the alternating, irregular, and discontinuous bands of dark grey dolostone, light grey saccharoidal dolomite rich in sphalerite, and white sparry dolomite. **B)** Fine-grained pale yellow sphalerite forming dense aggregates replacing the light grey saccharoidal dolomite; note the fine sphalerite veinlets crosscutting the dark grey dolostone (black arrow). Abbreviations: Host Do – host dolostone, Sacch Dol – saccharoidal dolomite; Sph – sphalerite.

recrystallized phase of previous dolomite. Fine-grained (0.02–0.04 mm in diameter), irregular-shaped pyrite is disseminated throughout the samples, but is preferential to the dolomite. Locally, it forms aggregates and is commonly altered to hematite. Galena forms large, irregular-shaped masses (5–8 mm long; trace to 3 volume %) that replace the host dolostone. It occurs as fine-grained, skeletal crystals interstitial to quartz and sphalerite grains (Fig. 20D) forming a network of small veinlets that are preferentially located in the darker dolostone bands and lenses. Galena is locally altered to cerussite ($PbCO_3$; Fig. 20E). Fine carbonate veinlets (calcite ±dolomite) that cut sphalerite (Fig. 20F) are subsequently cut by galena.

Munroe Deposit

Hand Samples

Samples from the Munroe deposit consist of irregular and discontinuous lenses and patches of fine-grained, dark grey dolostone intermingled with medium-grained, crystalline, light grey saccharoidal dolomite, and coarse-grained white sparry dolomite. Locally, these form a texture referred to as 'zebra' dolomite (Fig. 21A). Dense clusters of fine- to medium-grained, pale to dark yellow sphalerite form irregular lenses and patches that replace the saccharoidal dolomite (Fig. 21B). Sphalerite also occurs as individual grains or aggregates of grains disseminated in the dark grey dolostone and saccharoidal dolomite, and as veinlets crosscutting the dark grey dolostone (Fig. 21B). It is rarely associated with the white sparry dolomite that fills open spaces and pores. White barren carbonate veinlets crosscut all phases.

Mineralogy and Paragenesis

The paragenetic sequence of minerals in samples from the Munroe deposit is presented in Figure 22. The dark grey host dolostone is composed of fine-grained (0.02–0.15 mm in diameter; 20–50 volume %), anhedral dolomite crystals that form irregular lenses and patches. Generally, the host dolostone is not mineralized, but occasionally minor intergranular sphalerite and pyrite, most of which has been recrystallized, are observed (Fig. 23A). Stylolites and allochems remain from the original limestone.

The second phase of dolomite (15–40 volume %) is light grey and saccharoidal, and it replaces the dark grey dolostone. This dolomite consists of euhedral to subhedral, medium-sized (0.4–1 mm in diameter) crystals that are recrystallized. This dolomite contains most of the sulphide mineralization.

Pyrite (trace to 2 volume %) is very fine-grained (<0.01 mm in diameter) and is disseminated throughout the dark grey dolostone and the light grey saccharoidal dolomite as individual, subhedral to euhedral crystals closely associated with sphalerite. In some cases, pyrite forms angular aggregates in the light grey saccharoidal dolomite.

Fine-grained (0.1–0.4 mm in diameter) and irregular-shaped interstitial sphalerite is present in the host dolostone; however, most of the sphalerite mineralization occurs in the light grey saccharoidal dolomite as aggregates of equant, granular, yellow to brown, 0.2 to 0.8 mm grains. Alteration to smithsonite is visible along the edges of sphalerite grains. Sphalerite makes up about 10 to 25 volume % of the samples.

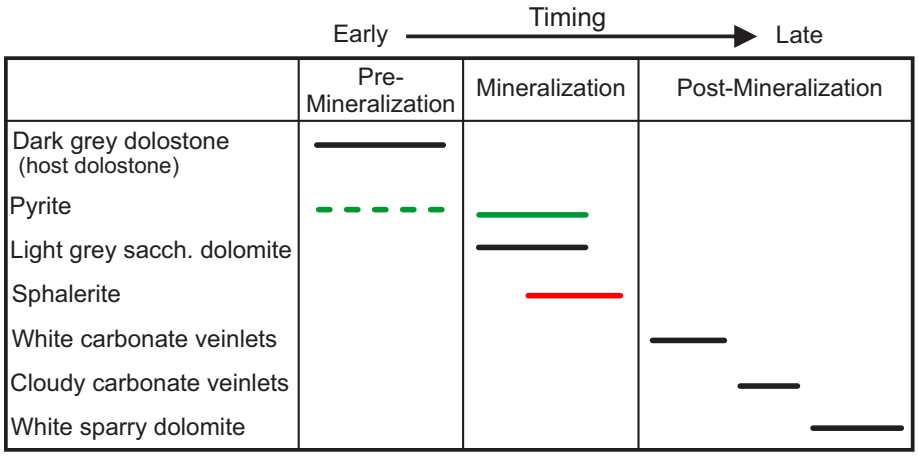

Figure 22. Simplified paragenetic sequence of minerals in samples from the Munroe deposit, British Columbia. Dashed lines refer to uncertainty in the precipitation timing of minerals. Abbreviation: sacch – saccharoidal.

Microcrystalline to fine-grained (<0.05 mm in diameter), white carbonate veinlets (trace volume %) crosscut the host dolostone, light grey dolomite, and sphalerite (Fig. 23B). These veinlets are subsequently crosscut by cloudy, microcrystalline carbonate veinlets.

A third dolomite phase occurs as white, coarse (0.8–2 mm in diameter), drusy, mosaic dolomite crystals (10–20 volume %) that fill open spaces and fractures. The grains are euhedral to subhedral and crystalline. This phase, which is not mineralized, crosscuts all other mineral phases.

Oldman Deposit

Hand Samples

Mineralized hand samples from the Oldman deposit are characterized by a large proportion of coarse crystalline, white- to cream-coloured calcite with variable amounts of sphalerite, galena, and pyrite, which occur as breccia-veins, fractures, and vug fillings (Fig. 24). Typically, sulphide minerals at Oldman occur as open space fillings in the breccia-veins. One sample is a dark grey fine- to medium-grained dolostone with disseminated sphalerite, and minor pyrite and galena. The dolostone is in gradational contact with a dark brown sphalerite-rich band (a few millimetres thick). Most of the sphalerite in the hand specimens is weathered to smithsonite.

Mineralogy and Paragenesis

The paragenetic sequence of minerals in samples from the Oldman deposit is presented in Figure 25. The host dolostone (10–50 volume %) is dark grey and consists of equant, subhedral to slightly interlocking, fine- to medium-sized dolomite grains (0.1–0.2 mm in diameter; Fig. 26A). The dolomite typically has irregular grain boundaries and contains up to 30 volume % microscopic fluid inclusions and semi-opaque inclusions of possible organic material. The dolostone is locally brecciated into 0.5 to 2 cm (diameter) sized

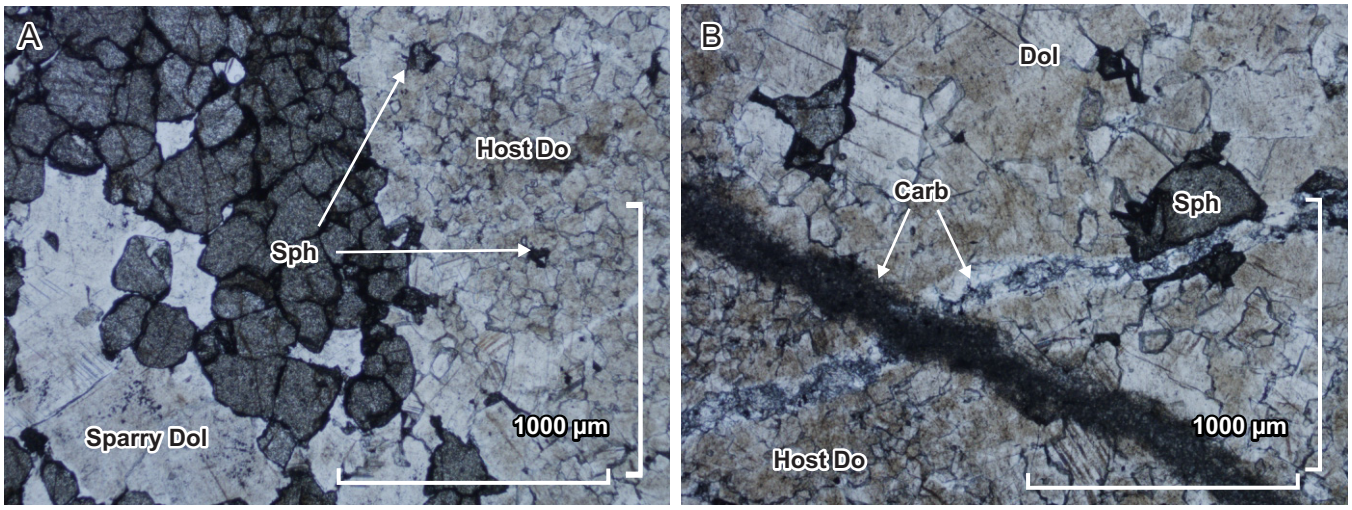

Figure 23. Photomicrographs showing the textural relationships of mineral phases in the Munroe deposit, British Columbia. **A)** Host dolostone with minor intergranular sphalerite adjacent to white sparry dolomite and granular sphalerite; plane polarized light (PPL). **B)** Carbonate veinlets crosscutting the host dolostone, light grey dolomite, and sphalerite. All crosscut by a cloudy carbonate veinlet; PPL. Abbreviations: Carb – carbonate; Dol – dolomite; Host Do – host dolostone; Sph – sphalerite.

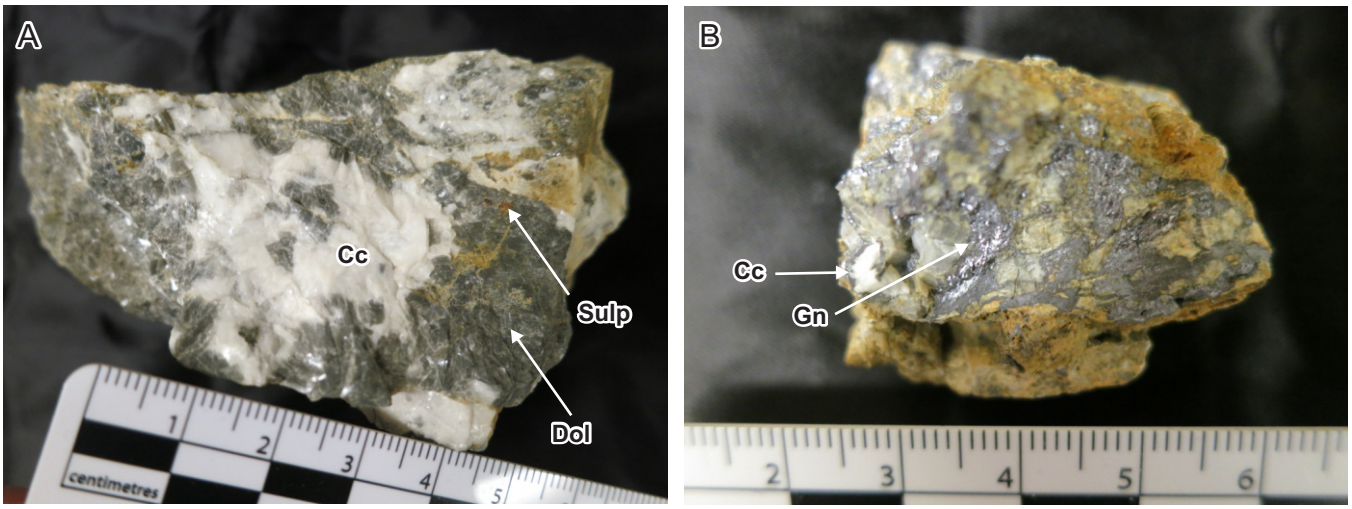

Figure 24. Hand samples from the Oldman deposit, Alberta. **A)** White coarse-grained calcite vein crosscutting coarse-grained crystalline grey dolomite; minor sulphide minerals fill fractures. **B)** Galena-calcite (±dolomite) vein. Abbreviations: Cc – calcite, Dol – dolomite, Gn – galena, Sulp – sulphides.

fragments, which show minor local replacement by sphalerite and pyrite.

Pyrite (trace to 50 volume %) occurs as fine- to medium-sized grains (0.02–0.6 mm in diameter). Very fine-grained pyrite (<0.04 mm in diameter) is also found disseminated throughout the samples and often outlines grain boundaries of sphalerite, or forms inclusions within sphalerite grains (Fig. 26B). These pyrite grains are typically irregular-shaped, sub-rounded, and oxidized to hematite.

Replacement sphalerite forms patches of granular aggregates of fine- to medium-grained (0.04–0.8 mm in diameter), yellow- to brown-coloured sphalerite. Sphalerite also occurs as disseminated, equant grains of a dark brown colour that are interstitial to the subhedral to slightly interlocking, equant grains of the host dolostone (Fig. 26C). Open space filling sphalerite that is medium- to coarse-grained (0.5–2.5 mm in diameter) and exhibits colloform textures (Fig. 26D, E) regularly surrounds the host dolostone fragments. All sphalerite (10–50 volume %) shows colour zonation (Fig. 26D, E) from dark red-brown in the core to yellow at the edge of grains. Sphalerite (Fig. 26F) and pyrite (Fig. 26G) are locally fractured, indicating that a brecciating event occurred subsequent to sulphide mineralization. Based on the relationships observed (Fig. 25), it is likely that pyrite (diagenetic) occurred first and continued to precipitate while sphalerite was introduced to the system, all of which was subsequently brecciated.

Late-stage medium- to very coarse-grained (0.5–15 mm in diameter), crystalline, euhedral white calcite (10–50 volume %) fills open spaces (e.g. veins, fractures, and vugs). Calcite crystals contain some very fine-grained (<0.04 mm in diameter), irregular-shaped pyrite and occasional fragmented sphalerite, but otherwise lack sulphide minerals. Cryptocrystalline calcite veinlets crosscut the coarser calcite phase.

Galena (trace to 10 volume %), the latest sulphide mineral, occurs mostly as large interstitial masses that fill spaces and fractures. It also replaces pyrite, sphalerite, and the host dolostone (Fig. 26H).

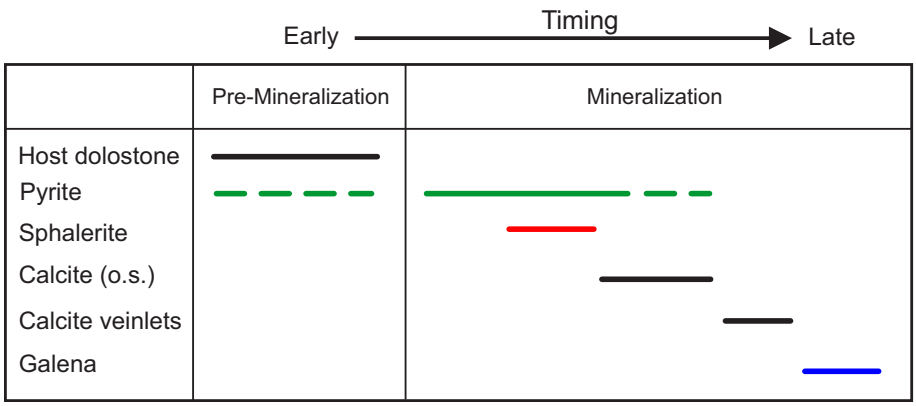

Figure 25. Simplified paragenetic sequence of minerals in samples from the Oldman deposit, Alberta. Dashed lines refer to uncertainty in the precipitation timing of minerals. Abbreviation: o.s. – open spaces (e.g. veins, fractures, and vugs).

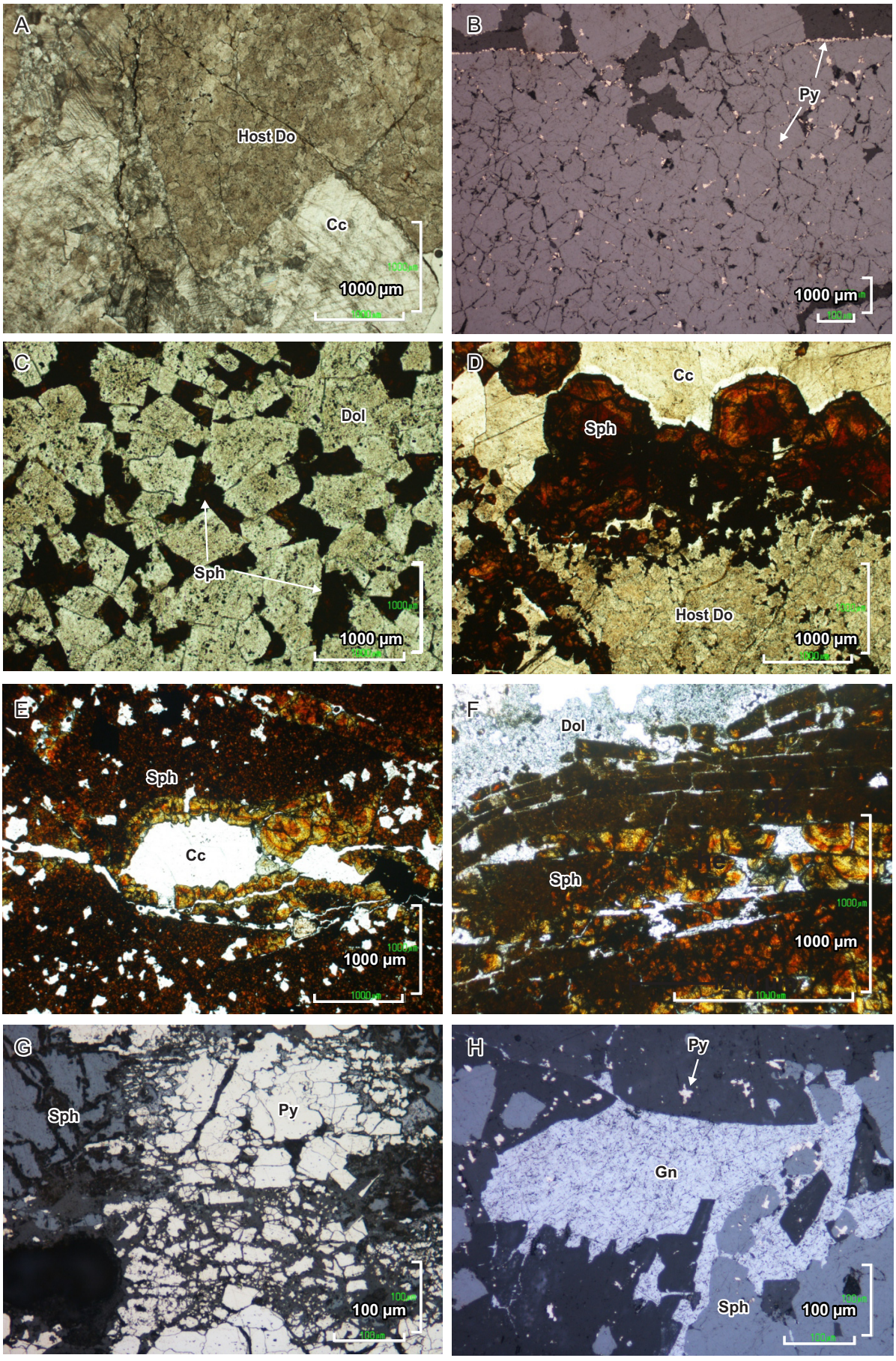
A
Host Do
Cc
1000 µm
B
Py
1000 µm
C
Dol
Sph
1000 µm
D
Cc
Sph
Host Do
1000 µm
E
Sph
Cc
1000 µm
F
Dol
Sph
1000 µm
G
Sph
Py
100 µm
H
Py
Gn
Sph
100 µm

SUMMARY OF OBSERVATIONS AND CONCLUDING REMARKS

The Monarch, Kicking Horse, Shag, Munroe, and Oldman carbonate-hosted sulphide deposits, southeastern Canadian Cordillera, share a consistent set of ore-forming elements, along with similar stratigraphic and structural controls. Collectively they have characteristics typical of MVT deposits and associated breccia-vein systems, especially in relation to mineralogy, texture and paragenesis (Leach and Sangster, 1993; Paradis et al., 2007). However, the Oldman deposit is slightly different than the other deposits in that its mineralization of sphalerite, galena and pyrite is associated with calcite (as oppose to dolomite in the other deposits) and occurs mainly as open-space fillings of breccia-veins, fractures and vugs, with minor replacement.

Ore-forming elements and controls

Depositional environment and tectonic setting

Many MVT deposits in the southeastern Canadian Cordillera, including Monarch, Kicking Horse and Shag, are located along major platform-to-basin facies transitions that existed at different times in the Paleozoic. Other deposits, such as Hawk Creek Zn-Pb, Mount Brussilof magnesite, and Red Mountain talc deposits, are also associated with this abrupt transition of shallow-water platformal carbonate to deeper water basinal facies.

The Monarch and Kicking Horse deposits are located along the Kicking Horse Rim, a fault-controlled, paleotopographic high that runs through the southern Rocky Mountains and over which transition from shallow-water platformal carbonate in the east to coeval complex succession of deep-water basinal and slope lithofacies to the west occurred (Aitken, 1971). This tectonic structure approximately corresponds to the projection of the Cathedral Escarpment at Monarch and Kicking Horse, and to the projection of the Eldon-Pika Escarpment at Shag. These escarpments have been interpreted as ancient submarine cliffs developed along the outer carbonate platform margin where large-scale synsedimentary mass wasting occurred during the Early Paleozoic (Stewart et al., 1993; Collom, 2009; Grasby et al., 2013). It is unclear what triggered the repeated collapses of the margin during the Early Paleozoic, but seismic activity in response to deep-seated faulting along the margin has been suggested by Stewart et al. (1993).

The proximity of the deposits and their frequency along the escarpments and the Kicking Horse Rim suggests that the carbonate platform-to-basin facies transitions and tectonic features influenced the formation of the deposits. This kind of paleotectonostratigraphic setting would have favoured the movement of mineralized fluids along the platform-basin transition and formation of hydrothermal mineral deposits and hydrothermal dolomitization.

Ore Controls

Basin-platform transition constitutes a significant control on the location of several carbonate-hosted deposits in southeast British Columbia. It is likely that this transition was the locus of deep-seated basement fault structures, and major and minor normal faults (Stewart et al., 1993; McMechan, 2012; Grasby et al., 2013; Johnston et al., 2017). Another important control is the host lithology and its porosity, which potentially influenced the depositional environment along the Kicking Horse Rim paleotopographic high and related unconformities (e.g. Aitken, 1971, 1997; Fritz and Simandl, 1993). All deposits occur in zones of high primary and secondary porosity (breccias, vugs, fractures, veins) associated with dolomite within the host dolostone.

The age of deposit formation is not well constrained. Those that have been dated using various high-precision paleomagnetic (Symons et al., 1998), biostratigraphic (Fritz and Simandl, 1993), microthermometric (Marshall et al., 2004; Vandeginste et al., 2007), and radiometric dating methods (e.g. U-Pb, U-Th in calcite, Rb-Sr in sphalerite, Ar-Ar and K-Ar in feldspar and clay minerals; Nesbitt and Muehlenbachs, 1994; Nelson et al., 2002; Vandeginste et al., 2007; Simandl et al., 2018) have ages that are contentiously debated, with estimates of the age of formation of the deposits and associated hydrothermal dolomitization ranging from Cambrian to Early Tertiary (Nesbitt and Muehlenbachs 1994; Powell et al., 2006; Vandeginste et al., 2007; Simandl et al., 2018).

Figure 26 (opposite page). Photomicrographs showing the textural relationships of mineral phases in the Oldman deposit, Alberta. **A)** Fragment of host dolostone composed of equant, subhedral to slightly interlocking, fine- to medium-grained dolomite in contact with coarse-grained calcite; plane polarized light (PPL). **B)** Massive aggregate of sphalerite with a minor train of pyrite along a sphalerite grain border and fine (<0.04 mm in diameter) disseminated pyrite; reflected light (RL). **C)** Medium-grained (0.04–0.8 mm in diameter) dark brown sphalerite interstitial to dolomite; PPL. **D)** Colloform sphalerite exhibiting colour zonation fills open spaces. Smaller grains are interstitial or replace the dolomite; PPL. **E)** Colloform sphalerite exhibiting colour zonation along the edges of cavity filled by calcite; PPL. **F)** Fractured sphalerite grains; RL. **F)** Fractured sphalerite grains; RL. **G)** Fractured pyrite grains; RL. **H)** Galena replacing sphalerite; RL. Abbreviations: Cc – calcite; Dol – dolomite; Gn – galena; Host Do – host dolostone; Py – pyrite; Sph – sphalerite.

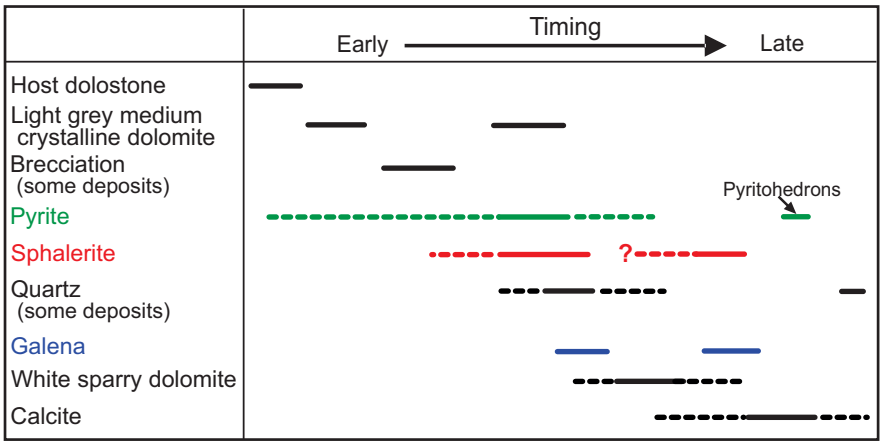

Figure 27. Generalized paragenesis for the studied deposits. Dashed lines and the interrogation mark refer to uncertainty in the precipitation timing of minerals.

Lithologies

All deposits are hosted in platformal dolomitized limestone, i.e., dolostone; however, they are not restricted to the same stratigraphic level. For example, Monarch and Kicking Horse occur mostly in the brecciated lower 125 metres of dolostone in the Middle Cambrian Cathedral Formation; Shag is hosted in sucrosic, vuggy, massive to brecciated dolostone of the Middle to Upper Cambrian Stephen, Eldon and Waterfowl formations that overlie the Cathedral Formation. Whereas the Munroe and Oldman deposits are in porous and brecciated dolostone of the Late Devonian Palliser Formation. Dolomitization is associated with mineralization, as the dolomitization is responsible for the generation of porosity (before mineralization and to a certain extent during mineralization) that prepared the rocks for mineralization.

Nature of mineralization

Mineralization is stratabound, forming clusters of individual orebodies that vary in character, shape (lenses, pods, disseminations, and veins), and continuity. At a smaller scale, sulphide mineralization occurs mostly as a replacement of the massive and brecciated host dolostone and as open-space fillings in breccia-vein systems. Typically, zones of highly brecciated and replaced dolostone are aligned in linear patterns that suggest a tectonic control.

All deposits have a simple ore mineral assemblage that consists of sphalerite, galena, and pyrite. Only Kicking Horse and Monarch, the largest of the deposits, contain chalcopyrite, silver, and barite. The gangue minerals, white sparry dolomite and coarse-grained calcite, are common in most deposits, with the exception of Oldman where the white sparry dolomite cement is absent. Quartz is intergrown with sulphide minerals at three of the showings at Shag (BM, C-4, and Red Bed), is rare at Monarch and Kicking Horse, and absent at Munroe and Oldman. This silicification of the matrix distinguishes Shag from the other deposits. Further study of carbonate-hosted sulphide deposits in the Rocky Mountain Foreland Belt and their geological characteristics is required to understand the significance and distribution of the silicification. However, a preliminary investigation suggests that the amount of silicification was probably dependent on the degree of fluid cooling that occurred during sulphide precipitation (Leach and Sangster, 1993).

Paragenesis

The paragenesis of minerals in the studied deposits is similar. As it is common for deposits within a district to exhibit a very similar mineral paragenesis (Leach et al., 2010), it is also expected for deposits occurring in the same geological environment to have a similar paragenesis. The paragenesis observed in this study varies from simple (e.g. C-3 showing) to complex (e.g. Monarch and Kicking Horse deposits). This may correspond to the size of deposit and the fact that the larger deposits are the result of multiple pulses of ore-forming hydrothermal fluids and cumulative superimposing events. In Figure 27, we present a generalized paragenesis for the studied deposits. The main petrographic features observed are as follows:

1. Mineralogy consists of sphalerite, galena, pyrite, dolomite, and calcite. Quartz is associated with sphalerite at the BM, C-4, and Red Bed showings of the Shag deposit, and is absent elsewhere (except for rare quartz at Kicking Horse). Chalcopyrite is only reported at Monarch in trace amounts (Goranson, 1937).
2. Dolostone hosts the sulphide mineralization. Several dolomite phases (replacement and cementation) are observed throughout the paragenesis and are associated with the sulphide mineralization (except at Oldman, where only dolomitization of the carbonate precursor is present):
   - Dolomitization of the limestone precursor preceded sulphide mineralization.
   - The host dolostone is replaced by a fabric-

destructive light grey medium crystalline dolomite (also referred to saccharoidal dolomite at Munroe), and subsequently replaced by sphalerite (±galena, pyrite). This is only observed at Monarch, Kicking Horse, and Munroe.

- The most recent dolomite phase is the coarse crystalline white dolomite cement filling the remaining open spaces after the main phase of sulphide mineralization. It is observed at Monarch, Kicking Horse, Munroe, BM, and C-3. At Oldman, coarse-grained white calcite cement (±traces of dolomite) fills the cavities and fractures.

3. A generalized sulphide mineral paragenesis is pyrite, followed by sphalerite and galena. Galena is the last sulphide to precipitate and occurs mainly as open-space filling.
4. A single phase of sphalerite precipitation is identified, except at Monarch and Kicking Horse where two phases are observed: in the first phase, sphalerite is finely disseminated in the dolostone and associated with pyrite.
5. Pyrite occurs intermittently in the paragenesis: first as very fine, diagenetic grains disseminated in dolostone (pre-mineralization), second as coarser grains and aggregates associated with sphalerite (mineralization stage), and third as coarse-grained pyritohedrons filling open spaces (post-mineralization).

NEXT STEPS

Preliminary petrographic study of the deposits provides information about their mineralogy, textures, and paragenesis. Additional petrographic work using cold-cathode cathodoluminescence will define the different carbonate phases and strengthen the paragenesis. Detailed micro-analytical analyses from selected samples will further constrain ore-forming processes, and the genetic links between these deposits and other carbonate-hosted deposits of the southeastern Canadian Cordillera (e.g. Mount Brussilof magnesite, Lead Mountain Zn-Pb, Hawk Creek Zn-Pb (±Ag), Steamboat (Zn-Pb), Rock Canyon Creek F-REE, and Silver Giant Ba-Zn-Pb).

In situ trace element analyses of sulphides and carbonates by laser ablation inductively coupled plasma mass spectrometry (LA ICP-MS), such as rare-earth elements and yttrium (REE+Y) content of carbonates and specialty metal content (e.g. Ge, Ga, In) of sulphide minerals, may be particularly revealing and provide insight into dolomite- and ore-forming fluid chemistry. Isotopic analyses (e.g. O, C, Sr, S, Pb) of sulphides, barite, and carbonates by bulk analytical techniques on handpicked grains and by high-precision in situ methods (LA-ICP-MS) will help constrain the sources of ore-forming fluids and metals in hydrothermal mineral deposits. Fluid inclusion microthermometry and evaporate mound analyses of ore and gangue minerals will provide information about the temperatures and salinities of formation of the mineralization. Pyrite and/or sphalerite Re-Os and Rb-Sr isotopic analyses are planned to help constrain the age of the sulphide mineralization. Age dating of accessory minerals (e.g. micas, apatite, rutile, monazite) hosted locally by sparry carbonate associated with the mineralization will also be attempted. If interpretable data is obtained, the dates will help to constrain the ages of MVT mineralization, sparry dolomitization, and other mineral deposit types in southeast British Columbia.

ACKNOWLEDGMENTS

This paper is a contribution to NRCan's Targeted Geoscience Initiative Program (TGI). Dr George Simandl and Carlee Akam of the British Columbia Ministry of Energy and Mines, Victoria are thanked for their critical review. The paper also benefited from the meticulous review of JoAnne Nelson of the British Columbia Geological Survey and Dr Neil Rogers of the Geological Survey of Canada. Page layout and final edits were completed by Elizabeth Ambrose.

REFERENCES

Aitken, J.D., 1971. Control of lower Paleozoic sedimentary facies by the Kicking Horse Rim, southern Rocky Mountains, Canada; Bulletin of Canadian Petroleum Geology, v. 19, p. 557–569.

Aitken, J.D., 1989. Birth, growth and death of the Middle Cambrian Cathedral carbonate lithosome, southern Rocky Mountains; Bulletin of Canadian Petroleum Geology, v. 37, p. 316–333.

Aitken, J.D., 1997. Stratigraphy of the Middle Cambrian platformal succession, southern Rocky Mountains; Geological Survey of Canada, Bulletin 398, 322 p.

Allan, J.A., 1914. Rocky Mountain section between Banff, Alberta, and Golden, B.C., along the Canadian Pacific Railway; Geological Survey of Canada, Summary Report for 1912, p. 165– 176.

Bending, D., 1979. Shag Claims, Rio Tinto Canadian Exploration Ltd.; British Columbia Assessment Report No.7382, 127 p.

Brown, W.L., 1948. Monarch and Kicking Horse Mines; Canadian Institute of Mining Symposium on Structural Geology of Canadian Ore Deposits, p. 231–237.

Collom, C.J., 2009. Evidence of syn-sedimentary tectonism in the Burgess Shale and other middle Cambrian units, British Columbia, Canada; Frontier + Innovation, Canadian Society of Petroleum Geologist, Canadian Society of Exploration Geophysicists, and Canadian Well Logging Society Convention, Calgary, Alberta, Canada, p. 1–5; https://www.geoconvention.com/archives/2009/232.pdf

Cook, D.G., 1975. Structural style influenced by lithofacies, Rocky Mountain main ranges, Alberta-British Columbia; Geological Survey of Canada, Bulletin 233, 73 p.

Cui, Y., Miller, D., Nixon, G., and Nelson, J., 2015. British Columbia digital geology; British Columbia Ministry of Energy and Mines, British Columbia Geological Survey, Open File 2015-2.

Evans, T.L., Campbell, F.A., and Krouse, H.R., 1968. A reconnaissance study of some western Canadian lead-zinc deposits; Economic Geology, v. 63, p. 349–359.

Fritz, W.H. and Simandl, G.J., 1993. New Middle Cambrian fossil and geological data from the Brussilof magnesite mine area, southeastern British Columbia, *In:* Current Research, Part A; Geological Survey of Canada, Paper 93-1A, p. 183–190.

Gibson, G., 1979a. Geology of the Munroe-Alpine-Boivin carbonate-hosted zinc occurrences; Rocky Mountain Front Ranges, southeastern British Columbia; British Columbia Ministry of Energy, Mines and Petroleum Resources, Preliminary Map No. 46.

Gibson, G., 1979b. Geological report on the SOAB 4 and SOAB 5 mineral claims within the Boivin Group, Fort Steele Mining Division, 82J/3E, 82J/14E; British Columbia Ministry of Energy, Mines and Petroleum Resources, Assessment Report 7489, 9 p.

Goranson, E.A., 1937. Geology of the monarch and kicking horse ore deposits, British Columbia; Economic Geology, v. 32, p. 471–493.

Graf, C., 1998. Petrography and chemical analysis of a suite of rock samples from the Oldman River lead-zinc prospect; Alberta Mineral Assessment Report 19970014, 20 p.

Grasby, S.E., Richards, B.C., Sharp, C.E., Brady, A.L., Jones, G.M., and Dunfield, P.F., 2013. The Paint Pots, Kootenay National Park, Canada—a natural acid spring analogue for Mars; Canadian Journal of Earth Sciences, v. 50, p. 94–108.

Hedley, M.S., 1954. Mineral deposits in the southern Rocky Mountains of Canada, *In:* Guidebook of Banff-Golden-Radium, (eds) J.C. Scott and F.C. Fox; Alberta Society Petroleum Geologists, 4th annual field conference guidebook, p. 110–118.

Hendrickson, G.A., 1988. Geophysical report on the Shag Creek project, Albert River area; British Columbia Ministry of Energy, Mines and Petroleum Resources, Assessment report 17814, 31 p.

Holter, M.E., 1977. The Oldman River lead zinc occurrence southwestern Alberta; Bulletin of the Canadian Petroleum Geology, v. 25, no.1, p. 92–109.

Jensen, S., 1991. Geochemical assessment report on the Shag property, Golden Mining Division; British Columbia Ministry of Energy, Mines and Petroleum Resources, Assessment Report 21885, 39 p.

Johnston, P.A., Collom, C.J., and Desjardins, P., 2017. Lower to Middle Cambrian of the southern Canadian Rockies, *In:* Geologic Field Trips of the Canadian Rockies, (ed.) J.C.C. Hsieh; 2017 Meeting of the Geological Society of America Rocky Mountain Section: Field Guide 48, p. 71–121.

Katay, F., 2017. Exploration and mining in the Southeast Region, British Columbia, *In:* Exploration and Mining in British Columbia, 2016; British Columbia Ministry of Energy and Mines, British Columbia Geological Survey, Information Circular 2017-1, p. 73–107.

Leach, D.L. and Sangster, D.F., 1993. Mississippi Valley-type lead-zinc deposits, *In:* Mineral Deposit Modeling, (ed.) R.V. Kirkham; Geological Association of Canada, Special Paper 40, p. 289–314.

Leach, D.L., Taylor, R.D., Fey, D.L., Diehl, S.F., and Saltus, R.W., 2010. A deposit model for Mississippi Valley-type lead-zinc ores, Chapter A *In:* Mineral Deposit Models for Resource Assessment: U.S. Geological Survey, Scientific Investigations Report 2010-5070-A, 52 p.

Lenters, M.H., 1981. Geological mapping and geochemical sampling, Shag Claims, Golden Mining Division; British Columbia Ministry of Energy, Mines and Petroleum Resources, Assessment Report 9678, 74 p.

Lenters, M.H., 1982. Report on diamond drilling, Shag Claims, Golden Mining Division; British Columbia Ministry of Energy, Mines and Petroleum Resources, Assessment Report 10143, 85 p.

Marshall, D., Simandl, G., and Voormeij, D., 2004. Fluid Inclusion evidence for the genesis of the Mt. Brussilof magnesite deposit, *In:* Industrial Minerals with Emphasis on Western North America, (eds) G.J. Simandl, W.J. McMilland, and N.D. Robinson; British Columbia Ministry of Energy and Mines, Paper 2004-2, p. 65–75.

McMechan, M.E., 2012. Deep transverse basement structural control of mineral systems in the southeastern Canadian Cordillera; Canadian Journal of Earth Sciences, v. 49, p. 693–708.

McMechan, M.E. and Leech, G.B., 2011a. Geology, Tangle Peak, British Columbia; Geological Survey of Canada, Canadian Geoscience Map 12, scale 1:50 000. https://doi:10.4095/287454

McMechan, M.E. and Leech, G.B., 2011b. Geology, Mount Peck, British Columbia; Geological Survey of Canada, Canadian Geoscience Map 9, scale 1:50 000. https://doi:10.4095/288765

McMechan, M.E. and Macey, E., 2012. Geology of the Rocky Mountains, west of Calgary, Alberta, in the Kananaskis west half map area (82J); Geological Survey of Canada, Scientific Presentation 13, 2012, 1 sheet. https://doi.org/10.4095/291576

Nesbitt, B.E. and Muehlenbachs, K., 1994. Paleo hydrogeology of the Canadian Rockies and origins of brines, Pb-Zn deposits and dolomitization in the Western Canada Sedimentary Basin; Geology, v. 22, p. 243–246.

Nesbitt, B.E. and Prochaska, W., 1998. Solute chemistry of inclusion fluids from sparry dolomites and magnesites in Middle Cambrian carbonate rocks of the southern Canadian Rocky Mountains; Canadian Journal of Earth Sciences, v. 35, p. 546–555.

Ney, C.S., 1954. Monarch and Kicking Horse Mines, Field, British Columbia, *In:* Guidebook of Banff-Golden-Radium, (eds) J.C. Scott and F.C. Fox; Alberta Society Petroleum Geologists, 4th annual field conference guidebook, p. 119–136.

Ney, C.S., 1957. Monarch and Kicking Horse mines, *In:* Structural Geology of Canadian Ore Deposits; Canadian Institute of Mining and Metallurgy, v. 2, p. 143–152.

Norris, D.K., 1993. Geology, Fording River, (East Half), West of Fifth Meridian, British Columbia-Alberta; Geological Survey of Canada, A Series Map 1831A, 1 sheet. https://doi.org/10.4095/192422

Pana, D., 2006. Unraveling the structural control of Mississippi Valley-type deposits and prospects in carbonate sequences of the Western Canada Sedimentary Basin, *In:* Potential for Carbonate-Hosted Lead-Zinc Mississippi Valley-Type Mineralization in northern Alberta and southern Northwest Territories: Geoscience Contributions, Targeted Geoscience Initiative, (ed.) P.K. Hannigan; Geological Survey of Canada, Bulletin 591, p. 255–304.

Paradis, S., Hannigan, P., and Dewing, K., 2007. Mississippi Valley-type lead-zinc deposits, *In:* Mineral Deposits of Canada: A Synthesis of Major Deposit-Types, District Metallogeny, the Evolution of Geological Provinces, and Exploration Methods, (ed.) W.D. Goodfellow; Geological Association of Canada, Mineral Deposits Division, Special Publication No. 5, p. 185–203.

Paradis, S. and Simandl, G.J., 2017. Is there a genetic link between the SEDEX and MVT deposits of the Canadian Cordillera?; *In:* Targeted Geoscience Initiative - 2016 Report of Activities, (ed.) N. Rogers; Geological Survey of Canada, Open File 8199, p. 107–113.

Paradis, S. and Simandl, G.J., 2018. Are there genetic links between carbonate-hosted barite-zinc-lead sulphide deposits and magne-

site mineralization in southeast British Columbia?; *In:* Targeted Geoscience Initiative: 2017 report of activities, volume 1, (ed.) N. Rogers; Geological Survey of Canada, Open File 8358, p. 217–227.

Powell, W.G., Johnston, P.A., Collom, C.J., and Johnston, K., 2006. Middle Cambrian brine seeps on the Kicking Horse Rim and their relationship to talc and magnesite mineralization and associated dolomitization, British Columbia; Economic Geology, v. 101, p. 431–451.

Price, R.A., 1994. Cordilleran tectonics and the evolution of the Western Canada Sedimentary Basin, Chapter 2 *In:* Geological Atlas of the Western Canada Sedimentary Basin, (eds) G. Mossop and I. Sheltsin; Alberta Research Council and Canadian Society of Petroleum Geologists, Calgary.

Salat, H.P., 1988. The Oldman River project (southwestern Alberta), geological report on exploration carried out in summer 1988; Rapparee Resources Ltd.; Alberta Energy, Mineral Assessment Report 19880001, 32 p.

Simandl, G.J. and Hancock, K.D., 1991. Geology of the Mount Brussilof magnesite deposit, southeastern British Columbia, *In:* Geological Fieldwork 1990; British Columbia Ministry of Energy, Mines and Petroleum Resources, Paper 1991-1, p. 269–278.

Simandl, G.J., Hancock, K.D., Fournier, M., Koyanagi, V.M., Vilkos, V., Lett, R., and Colbourne, C., 1992. Geology and major element geochemistry of the Mount Brussilof magnesite deposit, southeastern British Columbia, (82J/12m 13); British Columbia Ministry of Energy, Mines and Petroleum Resources, Paper 1992-14 .14 p.

Simandl, G.J., Petrus, J., Leybourne, M., and Paradis, S., 2018. Mount Brussilof fersmite — a time constraint on magnesite, MVT mineralization, dolomitization, and a Nb-REE hydrothermal event in SE British Columbia; Resources for Future Generations Resources for Future Generations 2018, Vancouver, British Columbia, June 16-21, 2018, Abstracts. http://www.rfg2018.org/

Stewart, W.D., Dixon, O.A., and Rust, B.R., 1993. Middle Cambrian carbonate-platform collapse, southeastern Canadian Rocky Mountains; Geology, v. 21, p. 687–690.

Symons, D.T.A., Lewchuk, M.T., and Sangster, D.F., 1998. Laramide orogenic fluid flow into the Western Canada Sedimentary Basin: evidence from paleomagnetic dating of the Kicking Horse Mississippi Valley-type ore deposit; Economic Geology, v. 93, p. 68–83.

Vandeginste, V., Swennen, R., Gleeson, S.A., Ellam, R.M., Osadetz, K., and Roure, F., 2007. Geochemical constraints on the origin of the Kicking Horse and Monarch Mississippi Valley-type lead-zinc ore deposits, southeast British Columbia, Canada; Mineralium Deposita, v. 42, p. 913–935.